Journal of Molecular Modeling (2022) 28: 197
https://doi.org/10.1007/s00894-022-05165-0

ORIGINAL PAPER

Electronic structure and reactivity indexes of cobalt clusters, both pure and mixed with *NO* and N_2O ($Co_n^q, q = 0, 1 \text{and } n = 4 - 9$)

José Guadalupe Facio-Muñoz[1] · David Alejandro Hernández-Velázquez[1] · Gregorio Guzmán-Ramírez[3] · Roberto Flores-Moreno[2] · J. G. Rodríguez-Zavala[1] · Francisco J. Tenorio[1]

Received: 30 September 2021 / Accepted: 19 May 2022 / Published online: 22 June 2022

Abstract

Among the most popular motivations for environmental scientists is improving materials that could be useful to fight or avoid pollution. This work shows a study of neutral and cationic cobalt clusters from 4 to 9 atoms (Co_n^q, $q = 0,1$ and $n =$ 4–9) to model their separate interaction with contaminant nitric and nitrous oxides. This study is within the framework of the density functional theory in the Kohn-Sham scheme by using *BPW91* functional and *6-311G* and *6-31G** basis sets to calculate global and local reactivity indexes. The effect of spin multiplicity is also determined. Results on the geometries of pure cobalt clusters agree with previously reported structures. Global minimum energy structures showed a marked preference towards the interaction of nitric and nitrous oxide molecules with cobalt clusters through chemisorptive dissociation, with the dissociation of the corresponding nitrogen oxide. Reactivity indexes reveal an even-odd alternate, which is related to electron counts. Moreover, the chemical potential is lowering after interaction with nitrogen oxides. The Fukui function illustrates the reactive zones with a high probability of chemisorption of more nitrogen oxide molecules.

Keywords Cobalt clusters · *NO* and N_2O dissociation · Density functional theory · Reactivity indexes

✉ Francisco J. Tenorio
jose.tenorio@academicos.udg.mx

José Guadalupe Facio-Muñoz
jose.facio@academicos.udg.mx

David Alejandro Hernández-Velázquez
david.hernandez@academicos.udg.mx

Gregorio Guzmán-Ramírez
gregorio.guzman@academicos.udg.mx

Roberto Flores-Moreno
r.flores@academicos.udg.mx

J. G. Rodríguez-Zavala
jaime.rzavala@academicos.udg.mx

[1] Departamento de Ciencias Exactas y Tecnología, Centro Universitario de los Lagos, Universidad de Guadalajara, Enrique Díaz de León 1144, Lagos de Moreno 47460, Jalisco, México

[2] Departamento de Química, Centro Universitario de Ciencias Exactas e Ingenierías, Universidad de Guadalajara, Blvd. Marcelino García Barragan 1421, esq. Calzada Olímpica, Guadalajara 44430, Jalisco, México

[3] Departamento de Estudios del Agua y la Energía, Centro Universitario de Tonalá, Universidad de Guadalajara, Av. Nuevo Periférico 555, Ejido San José Tatepozco, Tonalá 45825, Jalisco, México

Introduction

Emissions from human activities modify the concentrations of essential gasses, which causes a considerable change in the survival conditions. Notably, the records show that the atmospheric concentrations of important greenhouse gases have increased over the last two centuries [1]. Environmental pollution is, nowadays, one of the most critical topics for humankind. Many efforts guide the way to fix the already damaged ecosystem, all of them trying to achieve more sustainable development or lowering the impact caused by human activities. Anthropogenic reactive nitrogen has been increasing over the past two decades, often associated with waste industries generating clouds of environmental pollution that originate in combustion processes at high temperatures and in-car engines. In this sense, the nitrogen oxides (NO_x) present in those clouds of pollution involve reactions that harm human health. For example, nitric oxide (*NO*) and nitrous oxide (N_2O) are some of the many toxic molecules that can destroy ozone, besides being precursors of acid rain. The challenge for chemistry, physics, or materials science is setting the formation mechanism constituents of this pollution and, in this way, reduce or eliminate their formation.

This elimination usually involves a *selective catalytic reduction* (SCR) process, whose basis resides on the chemical reduction of the NO_x molecules using a metal-based catalyst with activated sites to increase the reduction reaction. A nitrogen-based reducing agent (reagent), such as ammonia or urea, selectively reacts with NO_x within a specific temperature range and in the presence of the catalyst and oxygen to reduce the NO_x into molecular nitrogen (N_2) and water vapor (H_2O) [2]. These reactions that occur in a wide temperature range accompany a significant increase in costs. These costs are mainly due to the large volumes of catalyst required for the reduction reaction [3]. Therefore, it is desirable to have better materials to reduce toxic molecules such as nitrogen oxides.

The exploration of the adsorption of nitrogen oxides on metallic surfaces [4] can constitute the initial step of understanding the corrosion processes. For example, Piskorz et al. [4] analyzed the catalytic reactivity of the spinel Co_3O_4 sample, where different stages are suggested in the decomposition of N_2O. The first step refers to the reaction of the oxide on active metal sites, followed by an oxygen diffusion on the metal surface, and finally recombination of atoms to form N_2 and O_2. In the last decades, the study of metallic clusters has received considerable attention mainly because their information makes them a model of great utility on this topic. In this sense, it is essential to understand the behavior of its electronic structure and hence its geometry. Quantum confinement and low-dimensional effects of the clusters allow a wide variety of structural and electronic behaviors to be analyzed that are generally not scalable [5]. The clusters are pretty sensitive to the addition or subtraction of a single atom; besides, the size of these particles allows the theoretical study efficiently with a low computational cost [6]. In this way, it is possible to apply various properties that they exhibit and which make them of great interest in processes of adsorption and catalysis of other molecules [7]. For example, in the literature, several experimental and theoretical studies exist on different transition metals that show the dissociative chemisorption of *NO* on surfaces such as *Rh*, *Cr*, *Fe*, and *Co* [8, 9]. The *Fourier-transform ion cyclotron resonance* (FT-ICR) is a technique that is usually followed by mass spectroscopy, which produces cationic rhodium ions (Rh_6^+) and reacting with nitric oxide [10]. This reaction leads to the dissociative chemisorption of the oxide and the formation of rhodium dioxide and rhodium tetraoxide, releasing nitrogen molecules. In other reports, theoretical studies were performed on clusters with one to six *Rh* atoms to study N_2O adsorption and dissociation [11]. In this case, N_2O molecule is bonded to bridge sites; hence, the decomposition of this oxide on the metal surface is performed. It is interesting how N_2O is decomposed through $N-O$ bond, forming N_2 and O as the final products. On the other hand, theoretical studies on structural properties of Ag_nRh clusters were performed to investigate the adsorption of *NO* on the surface of these systems [12]. In that work is observed a size-dependent reactivity, indicating that the *Rh* atom acts as a more active adsorption site for *NO* than *Ag*. In this sense, the Ag_n clusters doped with *Rh* increase the reactivity toward *NO* adsorption.

The investigation of the reaction of *NO* on cobalt clusters reports the competition of dissociative chemisorption against molecular chemisorption of *NO* using ionic techniques in the gas phase. It shows the nature of the *NO* structure chemisorbed on *Co* clusters by examining reactions of displacement with molecular oxygen [13, 14]. Other studies show the reactions of cobalt cluster cations with nitrous oxide and nitric oxide by FT-ICR mass spectrometry [15], where there is evidence of *NO* decomposition suggested by the loss of molecular nitrogen, therefore forming $Co_n^+(O)$. This fact indicates that clusters of the formula Co_n showed new properties not present in bulk or compact structures. The latter leads to interesting chemistry on the cluster's surface owing to the formation of stable oxide clusters and the decomposition of nitric oxide with the loss of molecular nitrogen. In an attempt to rationalize results, theoretical studies have been carried out by *density functional theory* (DFT) of the interaction of nitric oxide with *Co* clusters in a wide range of both structures and multiplicities, showing changes in reactivity as a function of size [16–18]. For example, Hanmura et al. clearly showed the dissociative chemisorption of two *NO* molecules on Co_n^+ (n = 3-10) [17] using a tandem mass spectrometer and DFT calculation.

Accordingly, full geometry optimizations of these systems are desirable in order to make a comparison between theoretical and experimental results. There is much to this chemistry that remains to be understood, in particular, how these reactions are in function of particle size and structure [16], since experimental results show that these clusters present an exciting change in reactivity as a function of the cluster size [15, 18]. Although the experiments carried out show the formation of these systems, as well as dissociation of the nitric and nitrous oxide with the interaction with the cobalt clusters, there are no reports about the calculations that show either reactivity and geometry of these small size clusters, which is the aim of the present work. Specifically, clusters between four and nine cobalt atoms are naked and interacting with a single *NO* and N_2O molecule. Additionally, both neutral and charged systems are studied. There were several spin configurations considered for each case. Therefore, to explain the behavior of the Co_n clusters (n = 4–9), a theoretical density functional study has been developed. The goal is to understand the reactivity and geometry of Co_n interacting with both *NO* and N_2O to offer a possible explanation for the dissociation of nitrogen oxides in these systems. In this work, the global and local reactivity indexes explain dissociative chemisorption and predict the subsequent addition of nitrogen oxides.

The remainder of this article is organized as follows: In the next section, the methodology used for calculations is presented. Later, molecular structural arrangements and global and local reactivity results are shown, in addition to the binding energies. Finally, a summary and conclusions are given.

Methodology

The geometry optimizations were performed in neutral and cation clusters for both naked and capped structures with *NO* or N_2O. Each structure was evaluated with several multiplicities (see Table 1). In the first stage, the minimum energy search was performed through *Gradient Embedded Genetic Algorithm* (GEGA) [19] in order to assure that the global minimum structure was found. This search of minimum energy structures was obtained through *VWN* functional [20] and *LANL2DZ* basis set for cobalt atoms [21] as well as *D95* basis set for nitrogen and oxygen atoms [22]. This level of theory is supported in previous work [23].

The second stage of the calculations involved an improvement in geometry and electronic structure. In this sense, the calculations were developed using the GAUSSIAN 09 [24] and GAUSSIAN 16 [25] computational packages. In this way, a calibration was made through several basis sets and functionals testing. Such functionals were *BP86* [26, 27], *BPW91* [26, 28], *PW91* [28, 29], *M05* [30], *M05-2X* [31], *M06* [32], *M06-2X* [32], and *M06-L* [33]. These functionals were combined with four basis sets *6-311G* [34], *DZVP* [35, 36], *LANL2MB* [21], and *SDD* [37]. This calibration, developed for *Co* cluster dimers, was based on the ionization potential results since it is possible to compare with the experimental values reported in the literature [38, 39].

The best approximation was provided by M06-L functional in combination with DZVP and SDD basis sets (see Table 2). However, convergence problems were obtained with the four *Co* atoms cluster. According to Table 2, the next level of theory with the best approximation is M05/DZVP; however, convergence problems persisted, in this case, with four *Co* atoms cluster interacting with *NO* molecule (it was suspected that the problem was in the basis sets). Therefore, it was decided to use the third basis set that offered the best results for experimental ionization potential, the 6-311G basis set. On the other hand, in line with Gutsev et al. [40] and Guzmán-Ramirez et al. [23], BPW91 is one of the most widely used functionals in small clusters of transition metals, especially in *Co* clusters. Consequently, the level of theory selected in this work to re-optimize the geometries found in the first search stage is BPW91/6-311G. To make a comparison of this level of theory and the use of polarization functions, at that same stage, a reoptimization of the structures was also carried out using the basis set 6-31G* [41, 42] with the same functional for the calculation of exchange and correlation energy.

Concerning the local reactivity indexes, Fukui functions were obtained as proposed by Yang and Parr [43] in a finite difference scheme through

$$f^{+}(\mathbf{r}) = \rho_{N+1}(\mathbf{r}) - \rho_{N}(\mathbf{r}), \quad (1)$$

Table 1 Multiplicities ($2S + 1$) utilized in the search for the minimum energy structure of the potential energy surface using GEGA

System	$2S + 1$ With GEGA	Structure multiplicity With lower energy
Co_4	1, 3, 5, 7, 9, 11, 13, 15	11
Co_4^+	2, 4, 6, 8, 10, 12, 14, 16	8
$Co_4(NO)$	6, 8, 10, 12	8
$Co_4^+(NO)$	7, 9, 11, 13	7
$Co_4(N_2O)$	5, 7, 9, 11	5
$Co_4^+(N_2O)$	6, 8, 10, 12	8
Co_5	6, 8, 10, 12, 14	12
Co_5^+	7, 9, 11, 13	11
$Co_5(NO)$	7, 9, 11, 13	7
$Co_5^+(NO)$	6, 8, 10, 12	8
$Co_5(N_2O)$	6, 8, 10, 12	6
$Co_5^+(N_2O)$	5, 7, 9, 11	11
Co_6	9, 11, 13, 15	15
Co_6^+	8, 10, 12, 14	14
$Co_6(NO)$	6, 8, 10, 12	12
$Co_6^+(NO)$	5, 7, 9, 11	9
$Co_6(N_2O)$	9, 11, 13, 15	9
$Co_6^+(N_2O)$	8, 10, 12, 14	10
Co_7	12, 14, 16, 18, 20	16
Co_7^+	11, 13, 15, 17, 19	15
$Co_7(NO)$	9, 11, 13, 15, 17	11
$Co_7^+(NO)$	6, 8, 10, 12, 14	12
$Co_7(N_2O)$	8, 10, 12, 14, 16	10
$Co_7^+(N_2O)$	7, 9, 11, 13, 15	7
Co_8	11, 13, 15, 17, 19	17
Co_8^+	10, 12, 14, 16, 18	18
$Co_8(NO)$	8, 10, 12, 14, 16	12
$Co_8^+(NO)$	7, 9, 11, 13, 15	15
$Co_8(N_2O)$	11, 13, 15, 17	11
$Co_8^+(N_2O)$	12, 14, 16, 18	14
Co_9	12, 14, 16, 18, 20	18
Co_9^+	13, 15, 17, 19, 21	19
$Co_9(NO)$	11, 13, 15, 17	17
$Co_9^+(NO)$	14, 16, 18, 20	14
$Co_9(N_2O)$	14, 16, 18, 20	14
$Co_9^+(N_2O)$	11, 13, 15, 17	15

The calculations were performed using VWN exchange-correlation functional [20] and *LANL2DZ* [21] basis set

Table 2 Calibration results obtained for *Co* neutral dimer with various DFT levels of theory

	BP86	BPW91	PW91	M05	M05-2X	M06	M06-2X	M06-L
6-311G	6.00	5.81	5.65	5.54	6.71	5.96	9.40	4.98
DZVP	7.47	7.26	7.34	6.58	7.47	6.66	7.36	6.51
LANL2MB	7.39	7.16	7.29	7.48	8.72	7.44	8.70	7.55
SDD	6.94	6.76	6.83	6.84	7.35	6.90	7.48	6.27

Ionization energy (*IE*) in eV. Experimental value [38, 39] 6.42 eV

$$f^{-}(\mathbf{r}) = \rho_N(\mathbf{r}) - \rho_{N-1}(\mathbf{r}) \tag{2}$$

and

$$f^{0}(\mathbf{r}) = \frac{\rho_{N+1}(\mathbf{r}) - \rho_{N-1}(\mathbf{r})}{2}, \tag{3}$$

where $\rho_{N+1}(\mathbf{r})$, $\rho_N(\mathbf{r})$ and $\rho_{N-1}(\mathbf{r})$ are the electron densities of the system with *N+1*, *N*, and *N-1* electrons, respectively. The vertical ionization energies (*IE*) and electron affinities (*EA*) were calculated as $IE = E_{cation} - E_{neutral}$, and $EA = E_{neutral} - E_{anion}$. The electron chemical potential (μ) for a *N*-electron system with an external potential $V(\mathbf{r})$ and total energy *E* is the partial derivative of the energy to the number of electrons at a constant external potential. μ is the negative of Mulliken's electronegativity definition, the negative mean of *IE* and *EA*, obtained through a finite difference approximation of $\left[\frac{\partial E}{\partial N}\right]_V$ [44, 45]

$$\mu = -\frac{(IE + EA)}{2} \tag{4}$$

Besides, the response of the system to charge donation (μ^-) and charge acceptance (μ^+) fundamentally drives the direction of flow of charge [46] and can be obtained through

$$\mu^- = -\frac{(3IE + EA)}{4} \tag{5}$$

and

$$\mu^+ = -\frac{(IE + 3EA)}{4} \tag{6}$$

This approach makes it possible to differentiate the charge addition from the charge subtraction in a system.

The calculation of chemical hardness [47], differentiating the chemical potential to the number of electrons at constant energy potential, equals to:

$$\eta = \left[\frac{\partial \mu}{\partial N}\right]_V \tag{7}$$

The electrophilicity index calculation was as [48]:

$$\omega = \frac{\mu^2}{2\eta} \tag{8}$$

Finally, in order to confirm the interaction between the different sizes of cobalt clusters and the *NO* and N_2O molecules, the calculation of the binding energies (E_b) was performed, understood as the energy difference between the compounds $Co_n^q(NO)$ and $Co_n^q(N_2O)$, and the energies of each species separately (Co^q, *N*, and *O*) [49], as shown in the following equations:

$$E_b\left[Co_n^q(NO)\right] = E\left[Co_n^q(NO)\right] - nE(Co^q) - E(N) - E(O) \tag{9}$$

$$E_b\left[Co_n^q(N_2O)\right] = E\left[Co_n^q(N_2O)\right] - nE(Co^q) - 2E(N) - E(O) \tag{10}$$

where *n*=4-9 and *q*=0-1.

Results

As mentioned before, in the first stage to search for structures with lower energy using the GEGA computational package [19], we considered different spin multiplicities ($M = 2S + 1$) in all calculations in order to find the most stable spin state for each system. The range of multiplicities taken into account was based on each predecessor system's minimum energy spin state. These multiplicities are indicated in Table 1.

This way, from the relative energies for each cluster and with each respective multiplicity, the minimum energy geometries were found for the different systems. The following section describes the geometrical structure, one of the most critical features of the clusters studied here.

Co_n and related structures

As mentioned in the Methodology section, the lowest energy structures found in the first stage were reoptimized under the *BPW91/6-311G* and *BPW91/6-31G** theory levels. Geometries obtained for neutral and cation structures naked and interacting with *NO* or N_2O are shown in Figs. 1, 2, 3, 4, 5, and 6, respectively; bond distances are indicated in angstroms (Å). These figures indicate the bond distances for the two levels of theory used in the second stage, BPW91/6-311G and BPW91/6-31G*. Numbers without parentheses are bond distances for the first level of theory, while

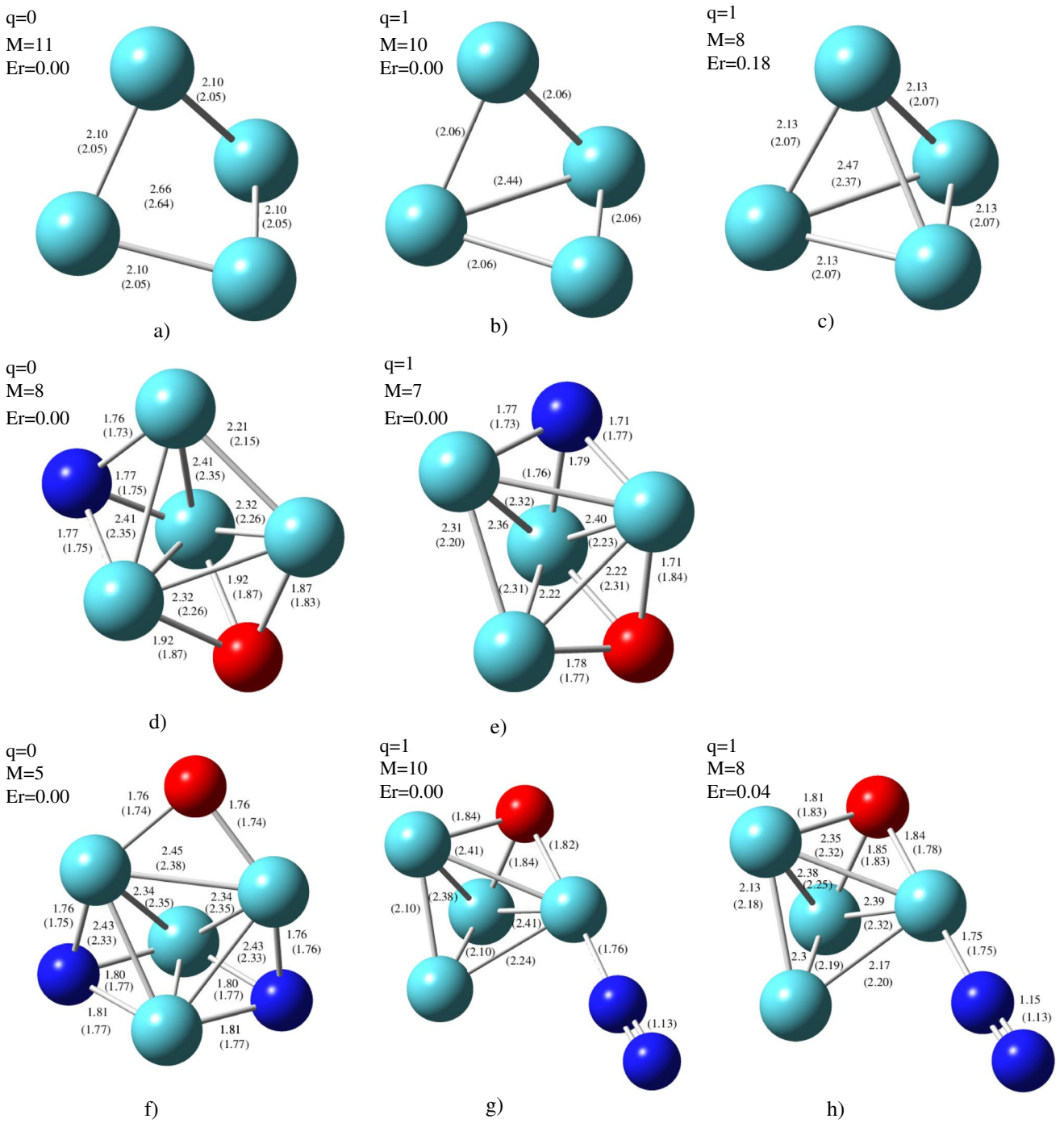

Fig. 1 Geometries obtained for Co_4^q, $Co_4^q(NO)$, and $Co_4^q(N_2O)$ (q = 0,1). Cobalt atoms are shown in blue green, nitrogen atoms in blue, and oxygen atoms in red. The distances are given in angstroms, *BPW91/6-311G* without parentheses and *BPW91/6-31G** with parentheses. $M = 2S + 1$, q is the electron charge, and E_r the relative energy in eV using *6-31G** basis set

parentheses are used for the second. q indicates the electron charge, M defines the multiplicity of the lowest energy cluster, and E_r is the relative energy in eV for the 6-31G* basis set.

For n=4, at both levels of theory, a tetrahedral structure is obtained with a spin multiplicity of 11 for neutral (see Fig. 1a). For the cation, the structures shown in Fig. 1b and c were obtained. With the 6-31G* basis set, the lowest energy geometry shown in part b was obtained with a multiplicity of 10; the second structure is shown in part c with a multiplicity of 8 (E_r= 0.18 eV). This last geometry also corresponds to the minimum energy obtained with the 6-311G basis set.

q=0
M=14
Er=0.00

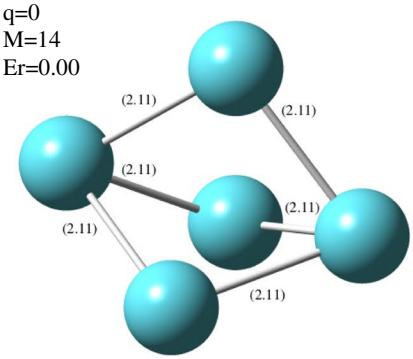

a)

q=0
M=12
Er=0.65

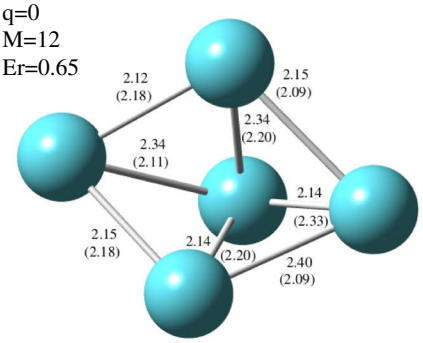

b)

q=1
M=11
Er=0.00

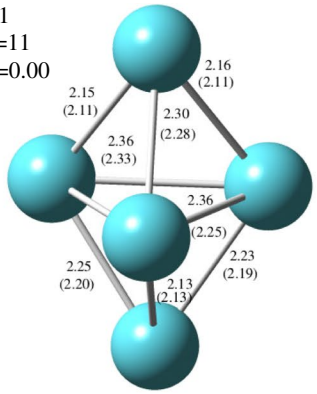

c)

q=0
M=7
Er=0.00

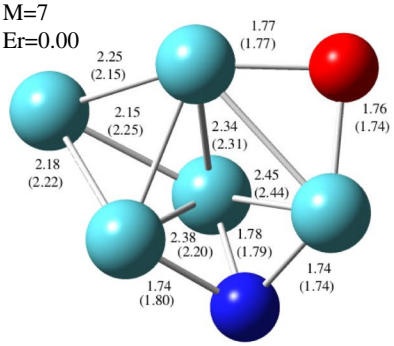

d)

q=1
M=10
Er=0.00

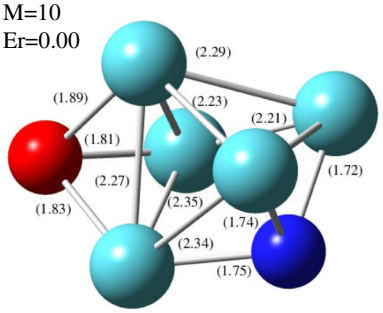

e)

q=1
M=8
Er=0.17

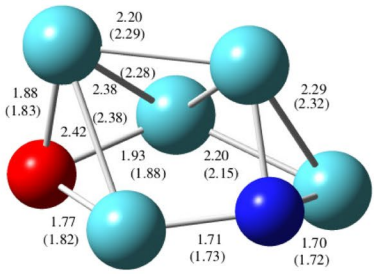

f)

q=0
M=8
Er=0.00

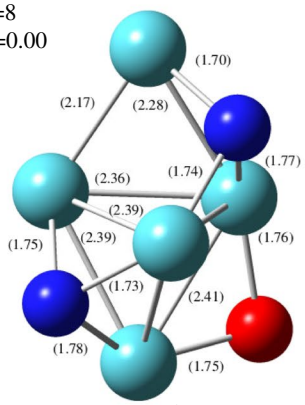

g)

q=0
M=6
Er=0.08

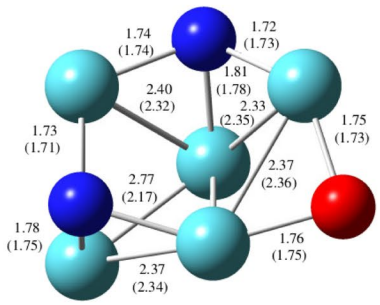

h)

q=1
M=9
Er=0.00

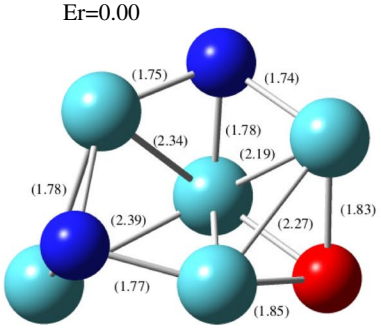

i)

q=1
M=11
Er=0.54

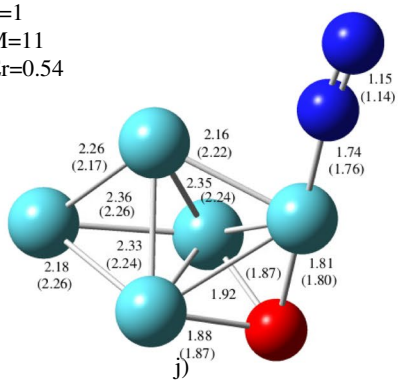

j)

◂**Fig. 2** Geometries obtained for Co_5^q, $Co_5^q(NO)$, and $Co_5^q(N_2O)$ (q = 0,1). Cobalt atoms are shown in blue green, nitrogen atoms in blue, and oxygen atoms in red. The distances are given in angstroms, *BPW91/6-311G* without parentheses and *BPW91/6-31G** with parentheses. $M = 2S + 1$, q is the electron charge, and E_r the relative energy in eV using *6-31G** basis set

It is essential to mention that these geometries are in good agreement with other reports obtained for neutral clusters [17, 50]; those references used a tandem mass spectrometer and DFT calculation besides multicanonical basin hopping method, respectively (see Fig. 1). It is interesting to see that geometry is according with the structure of other metal clusters since in a previous study based on density functional theory [51], for this size of a cluster of *Ni* atoms, the same atomic arrangement is presented. For $Co_4(NO)$, $Co_4^+(NO)$, and $Co_4(N_2O)$, both basis sets (6-31G* and 6-311G) coincide in the multiplicities as well as in the lowest energy structures (see Fig. 1d, e, and f). The lowest energy structure when interacting with both *NO* and N_2O shows no bonding between *N* and *O* atoms. This latter confirms dissociative chemisorption. Privileged positions for nitrogen and oxygen atoms are between cobalt atoms. Spin multiplicity decreases compared with naked cobalt clusters, suggesting that oxygen and nitrogen fill some electron shells. For *NO* interaction, this effect lowers *M* to 8 and 7 for neutral and charged clusters, respectively. It is more evident for the neutral cluster with N_2O since it lowers multiplicity to 5 for the neutral one. The lowest energy geometry for $Co_4^+(N_2O)$ via the basis set 6-31G*, shown in Fig. 1g, has a spin multiplicity of 10. With this same basis set, a similar structure is obtained with an energy difference of 0.04 eV and M=8. This system coincides geometrically with the one obtained by 6-311G (M=8), as shown in Fig. 1h. It is clear that using both basis sets, $Co_4^+(N_2O)$ structure shows an arrangement of $Co_4^+(O)$ bonded to a pair of *N* atoms, which are lightly symmetric.

In the case of n=5 the lowest energy structure obtained using the 6-31G* basis set for the neutral case has a multiplicity of 14 (Fig. 2a), which is the same geometry as that obtained with a multiplicity of 12 (Fig. 2b), except that they have an energetic difference of 0.65 eV respectively. This second structure of Co_5, in addition to geometrically matching the energy minimum obtained using the 6-311G basis set, also matches the size of the multiplicity, which is shown in Fig. 2b. For Co_5^+, the re-optimization calculations using the basis sets mentioned above agree that the energy minimum has a multiplicity of 11, both with a triangular bipyramid shape (see Fig. 2c). Previous reports for naked structures agree with that presented here [50]. For *NO* interaction, with both 6-31G* and 6-311G, a geometry with M=7 is obtained, where the dissociative chemisorption of *NO* on the cluster surface is evident (see Fig. 2d). Regarding $Co_5^+(NO)$, Figs. 2e and 2f present minima with a multiplicity of 10 and 8 with 6-31G*. Geometry with the multiplicity of 8 for that basis set turns out to be the same as that obtained when using 6-311G. In both cases, neutral and cation, the lowest energy isomers always show dissociative chemisorption of *NO*, where also, nitrogen and oxygen atoms occupy intermediate positions between cobalt atoms. Concerning their spin multiplicity, there is a sensitive lowering, understood in terms of filling electron shells through *N* and *O* atoms. For $Co_5(N_2O)$, the lowest energy structure found with 6-31G* has a multiplicity of 8, as shown in Fig. 2g. A second geometry for this system, with an energy of 0.08 eV higher than the previous one (M=6), corresponds to the minimum energy found with 6-311G (see Fig. 2h). The calculations made for $Co_5^+(N_2O)$ with 6-31G* yield two possible energy minima with multiplicities of 9 and 11 with an energy difference of 0.54 eV. The geometry with a multiplicity of 11 is the most energetically favored with 6-311G (see Fig. 2j). In addition to the N_2O dissociative chemisorption on the cluster surface, a possible N_2 formation is observed for the last structure.

For n=6, Fig. 3 shows that the neutral naked cluster (M =15) prefers a square bipyramidal structure [50]. A minimum distortion is due to the effect of the charge (M =14, see Fig. 3). Interaction with *NO* lowers (M =12 for neutral and 9 for cation) multiplicity. It is worth mentioning that the dissociative chemisorption of said nitrogen oxides is evident in the interaction of this cluster size with both *NO* and N_2O. According to Fig. 3, minima found with both basis sets coincide in structural arrangements and multiplicity for the minimum energy structures of these systems.

The results for Co_7 suggest two different lower energy structures calculated by 6-31G*, which have an energy difference of 0.37 eV (see Fig. 4a and b) and the same spin multiplicity. The geometry shown in Fig. 4b is also obtained as the minimum energy for calculations performed by 6-311G. For that basis set, it is clear that the most stable structure for Co_7 cluster corresponds to a pentagonal bipyramid having a spin multiplicity of 16, as presented in Fig. 4. Moreover, the number of unpaired electrons found in this work is the same as a result reported by Hong and coworkers [52]. It is important to note that this geometry also agrees with the reported by Zhan [50], Aguilera-Granja, and coworkers [52, 53]. In addition, as mentioned in the literature, the geometry of the small cluster is highly symmetric [53] such as that happening with this geometry. For the cation, the study with the polarized function suggests two structures as energy minima, which differ by 0.47 eV, as shown in Fig. 4c and d. Anew, the second isomer coincides with the minimum found when using the 6-311G basis set. For Co_7^+ (with a spin multiplicity equal to 15), the results show a geometry quite similar to the neutral case; in other words, no distortion exists when an electron is removed (see Fig. 4). On the other hand, the most favored structure for $Co_7(NO)$ system has a multiplicity of 11 (for both basis sets 6-31G* and 6-311G). This fact suggests

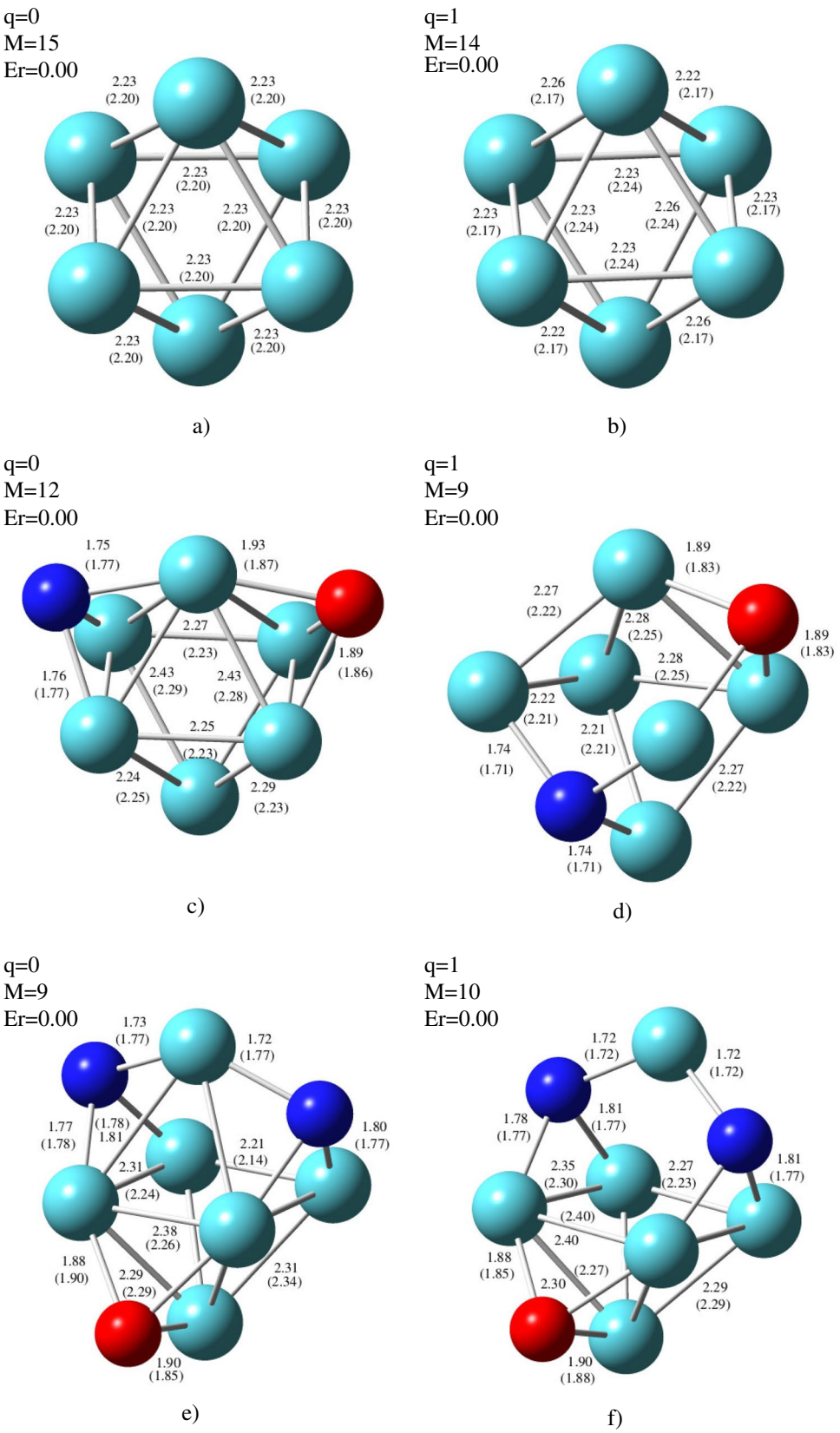

Fig. 3 Geometries obtained for Co_6^q, $Co_6^q(NO)$, and $Co_6^q(N_2O)$ (q = 0,1). Cobalt atoms are shown in blue green, nitrogen atoms in blue, and oxygen atoms in red. The distances are given in angstroms, *BPW91/6-311G* without parentheses and *BPW91/6-31G** with parentheses. $M = 2S + 1$, q is the electron charge, and E_r the relative energy in eV using *6-31G** basis set

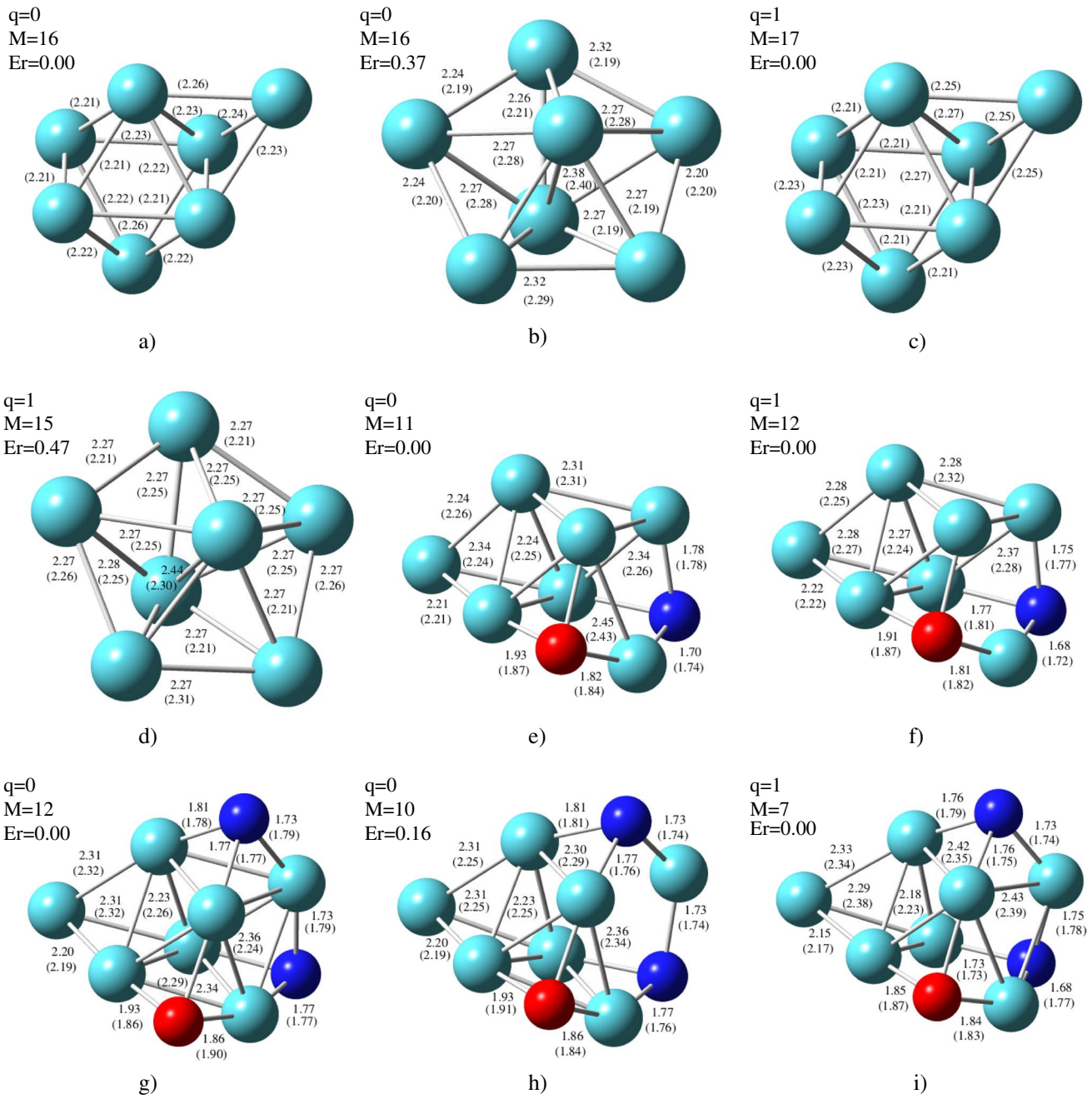

Fig. 4 Geometries obtained for Co_7^q, $Co_7^q(NO)$, and $Co_7^q(N_2O)$ (q = 0,1). Cobalt atoms are shown in blue green, nitrogen atoms in blue, and oxygen atoms in red. The distances are given in angstroms, *BPW91/6-311G* without parentheses and *BPW91/6-31G** with parentheses. $M = 2S + 1$, q is the electron charge, and E_r the relative energy in eV using the *6-31G** basis set

that the molecule of *NO* decreases the multiplicity. For this geometry, Fig. 4 shows that the *NO* molecule has been dissociatively chemisorbed. Additionally, Co_7 distorts due to its interaction with the *NO*. Cation $Co_7^+(NO)$ has a multiplicity equal to 12, and there is no bond between *N* and *O*, geometrically coinciding in both basis sets used in this work. In this case, the multiplicity increases in one unit, suggesting the effect of losing an electron. In the same manner as in Co_7, the geometry of the cation $Co_7^+(NO)$ is similar to $Co_7(NO)$. For the interaction with N_2O, the calculations made with 6-31G* suggest two lower energy isomers, although structurally quite similar, whose multiplicities are 12 and 10. The geometry with M=10 is the most favored (Fig. 4h) for the re-optimization performed with 6-311G. With either basis set, the lowest energy structure for $Co_7(N_2O)$ showed the *N* and *O* atoms chemisorbed on the center of opposite faces of

q=0
M=17
Er=0.00

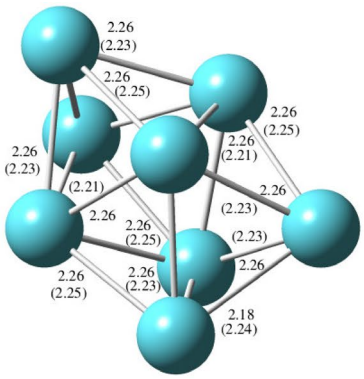

a)

q=1
M=18
Er=0.00

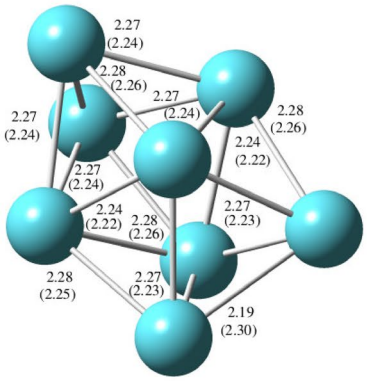

b)

q=0
M=12
Er=0.00

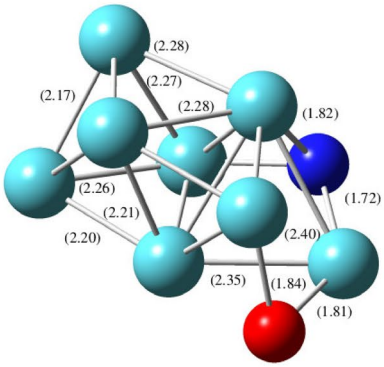

c)

q=0
M=12
Er=0.11

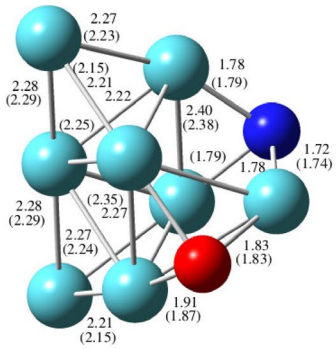

d)

q=1
M=13
Er=0.00

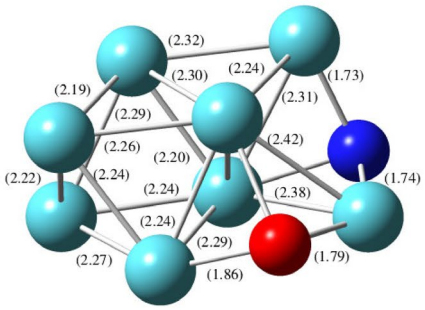

e)

q=1
M=15
Er=0.16

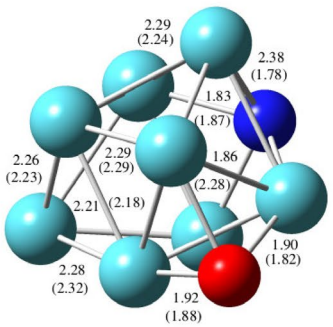

f)

q=0
M=11
Er=0.00

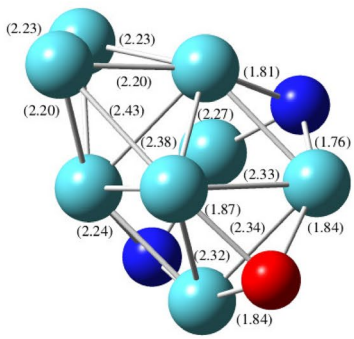

g)

q=0
M=11
Er=0.29

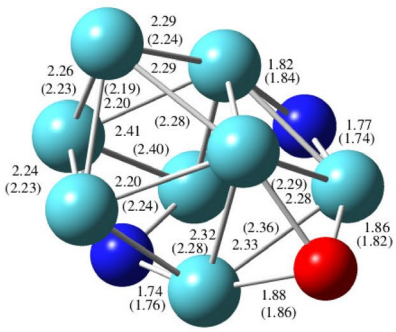

h)

q=1
M=14
Er=0.00

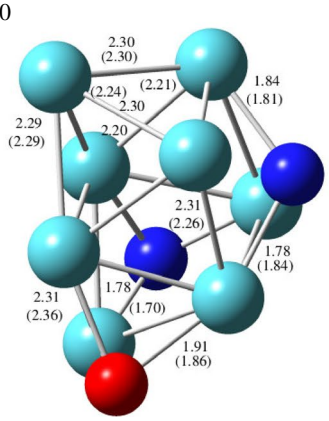

i)

Fig. 5 Geometries obtained for Co_8^q, $Co_8^q(NO)$, and $Co_8^q(N_2O)$ (q = 0,1). Cobalt atoms are shown in blue green, nitrogen atoms in blue, and oxygen atoms in red. The distances are given in angstroms, *BPW91/6-311G* without parentheses and *BPW91/6-31G** with parentheses. $M = 2S + 1$, q is the electron charge, and E_r the relative energy in eV using *6-31G** basis set

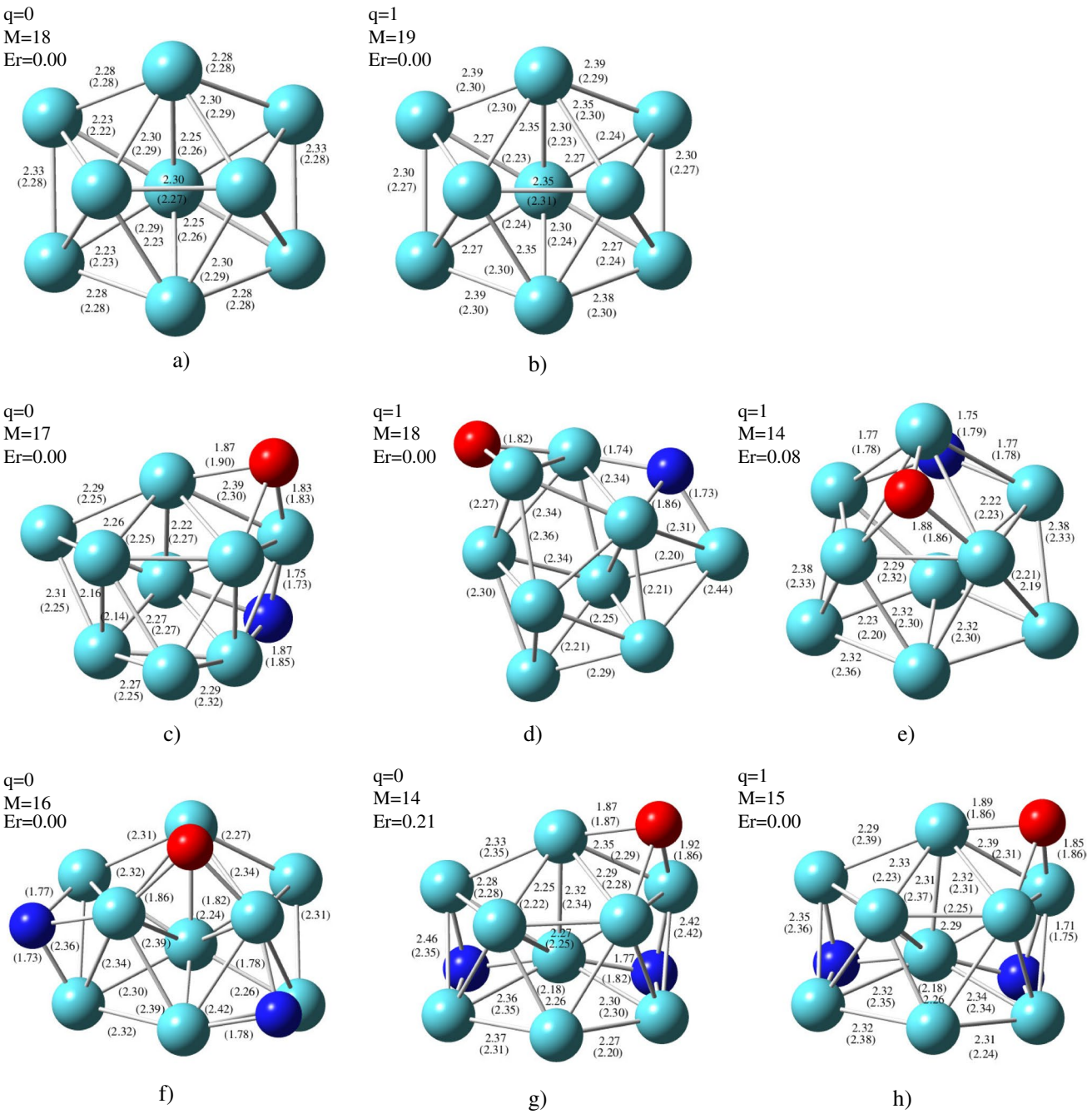

Fig. 6 Geometries obtained for Co_9^q, $Co_9^q(NO)$, and $Co_9^q(N_2O)$ (q = 0,1). Cobalt atoms are shown in blue green, nitrogen atoms in blue, and oxygen atoms in red. The distances are given in angstroms, *BPW91/6-311G* without parentheses and *BPW91/6-31G** with parentheses. $M = 2S + 1$, q is the electronic charge, and E_r the relative energy in eV using *6-31G** basis set

the geometry of Co_7 cluster. For the cationic composition of $Co_7^+(N_2O)$, Fig. 4 indicates that the most stable structure shows a multiplicity of 7 where dissociative chemisorption of N_2O (for both basis sets involved in this study) occurs; also, a significant similarity with the structure of $Co_7(N_2O)$ is observed, suggesting a poor structural effect due to ionization of the neutral system.

Figure 5 shows the geometries for the pure eight-atom *Co* cluster and interacting with *NO* and N_2O. The geometry of the Co_8 system (with a multiplicity of 17) agrees with that reported in the literature [50, 54]. According to Fig. 5a, the results obtained with 6-31G* and 6-311G agree in both M and molecular geometry, suggesting that there is no effect of polarization on this system. It is worth saying

that multiplicity increases one unit concerning the system of seven atoms. In addition, the total spin agrees with the result obtained by Hong [52]. The geometry of this system suggests a growth pattern of the cluster from Co_7 to Co_8 incorporating atoms, one by one, such as that shown by Rodríguez López et al. [53]. Co_8^+ with a spin multiplicity of 18 keeps the same geometry as the neutral case, which suggests no distortion after removal of one electron of the system. Once again, the results with both basis sets agree. The polarized function finds the geometries in Fig. 5c and d as energy minima for $Co_8(NO)$, both with M=12. The second isomer agrees with the minimum found by 6-311G; the minimum reported has a multiplicity of 12, decreasing considerably regarding the pure system. Also, as shown in Fig. 5, the nitric oxide molecule has no direct bond between N and O, suggesting a fragmentation of the molecule. NO considerably modified the Co_8 cluster original arrangement. The calculations made with 6-31G* suggest the geometry shown in Fig. 5e as the most stable for the one shown in Fig. 5f, also differing in the value of the electronic spin multiplicity. However, the 6-311G finds that for the cation, $Co_8^+(NO)$ with a multiplicity of 15, slight distortions are noticed relative to the neutral (see Fig. 5). The results obtained for the interaction of Co_8 and N_2O show two structures as energy minima with 6-31G* where, according to Fig. 5, there is an energy difference of 0.29 eV. Of these geometries, the one with the highest energy agrees with the structure representing the most stable system for the calculations performed with 6-311G (Fig. 5h). The $Co_8(N_2O)$ system with a multiplicity of 11 shows a dissociation of N_2O molecule. A similar structure is $Co_8^+(N_2O)$, with a spin multiplicity equal to 14, where the dissociative chemisorption of N_2O is clear on different faces of the cobalt cluster; that geometry turns out to be the most stable for both basis sets and even with the same multiplicity.

The minimums found on the potential energy surface for Co_9, Co_9^+, $Co_9(NO)$, $Co_9^+(NO)$, $Co_9(N_2O)$, and $Co_9^+(N_2O)$ are shown in Fig. 6. The structure obtained for Co_9 with a multiplicity of 18 is quite similar to the reported earlier by Zhan, and other works [50, 53]. Anew, regarding neutral systems described before, the growth pattern for this system suggests incorporating atoms one by one [53]. When Co_9^+ is ionized, results suggest that the structure with more energy stability has a multiplicity of 19 and a similar geometry to the neutral. The results obtained by 6-31G* and 6-311G suggest that both energy minima agree on the value of the electronic multiplicity and the geometry for this cluster size. Anew, the two levels of theory used in this work agree on the energy minimum for the structural arrangement of $Co_9(NO)$ (M = 17). With different structures and multiplicities for $Co_9^+(NO)$, the polarized basis set finds the geometries shown in Fig. 6d and e, the latter being the one that agrees with the most stable structure with 6-311G. For both the neutral system and the cation, those systems indicate dissociative chemisorption of NO, with the atoms adsorbed on centers of the faces of the original Co_9 geometry. In both cases, O and N atoms are chemisorbed on opposite sides of the cluster, differing considerably in structure (neutral and cation).

Finally, the $Co_9(N_2O)$ system has a multiplicity of 14 and is shown in Fig. 6 for the minimum energy with 6-311G. This geometry corresponds to the second minimum energy isomer obtained with 6-31G* since the first, with a multiplicity of 16, shows an entirely different structural arrangement. For both levels of theory, this geometry shows dissociative chemisorption of nitrous oxide, where N and O atoms form bridges on Co_9 atoms.

The cation of this composition exhibits a multiplicity of 15, for the results with both basis sets. For this system, Fig. 6 shows a distortion for this cationic state compared to the neutral state, thus indicating the effect of ionizing the system.

Global reactivity indexes

This section summarizes the results obtained for all neutral systems about the global reactivity indexes, such as ionization potential, also called ionization energy (IE), electron affinity (EA), chemical potential (μ), donor chemical potential (μ^-), acceptor chemical potential (μ^+), chemical hardness (η), and electrophilicity index (ω), all given in eV (see Fig. 7). The data for this properties can be also found in Table S13. The calculations were performed through the BPW91/6-311G and BPW91/6-31G* levels of theory, which are blue and orange boxes in Fig. 7, respectively.

For both basis sets used in this work, all clusters present positive values of ionization potential. Except $Co_6(N_2O)$, it is clear that the IE obtained with 6-31G* is more significant than that with the other basis set for each system analyzed. Examining Co_4, $Co_4(NO)$, and $Co_4(N_2O)$ clusters, there is a diminishing going from the first to the second, but an increase when the cluster is interacting with N_2O. In the systems with five cobalt atoms, the lowest ionization potential corresponds to the pure cluster. This property increases when NO and N_2O are present, according to the blue boxes, which indicate the results with 6-311G. In the case of six cobalt atoms, $Co_6(NO)$ has the lowest ionization potential. The $Co_6(N_2O)$ presents the most considerable stability since more energy is required to form a cation. Regarding the systems with seven atoms of cobalt, IE increases when Co_7 interacts with both NO and N_2O. This fact suggests that it is necessary to have more energy to remove an electron of the $Co_7(N_2O)$ system, which indicates that the nitrous oxide gives stability to the system concerning this descriptor. According to the results obtained for the clusters of eight atoms of cobalt (pure and mixed with NO and N_2O), it is observed that $Co_8(NO)$ becomes less susceptible to positive ionization. In Fig. 7, the IE of $Co_9(NO)$ is much higher

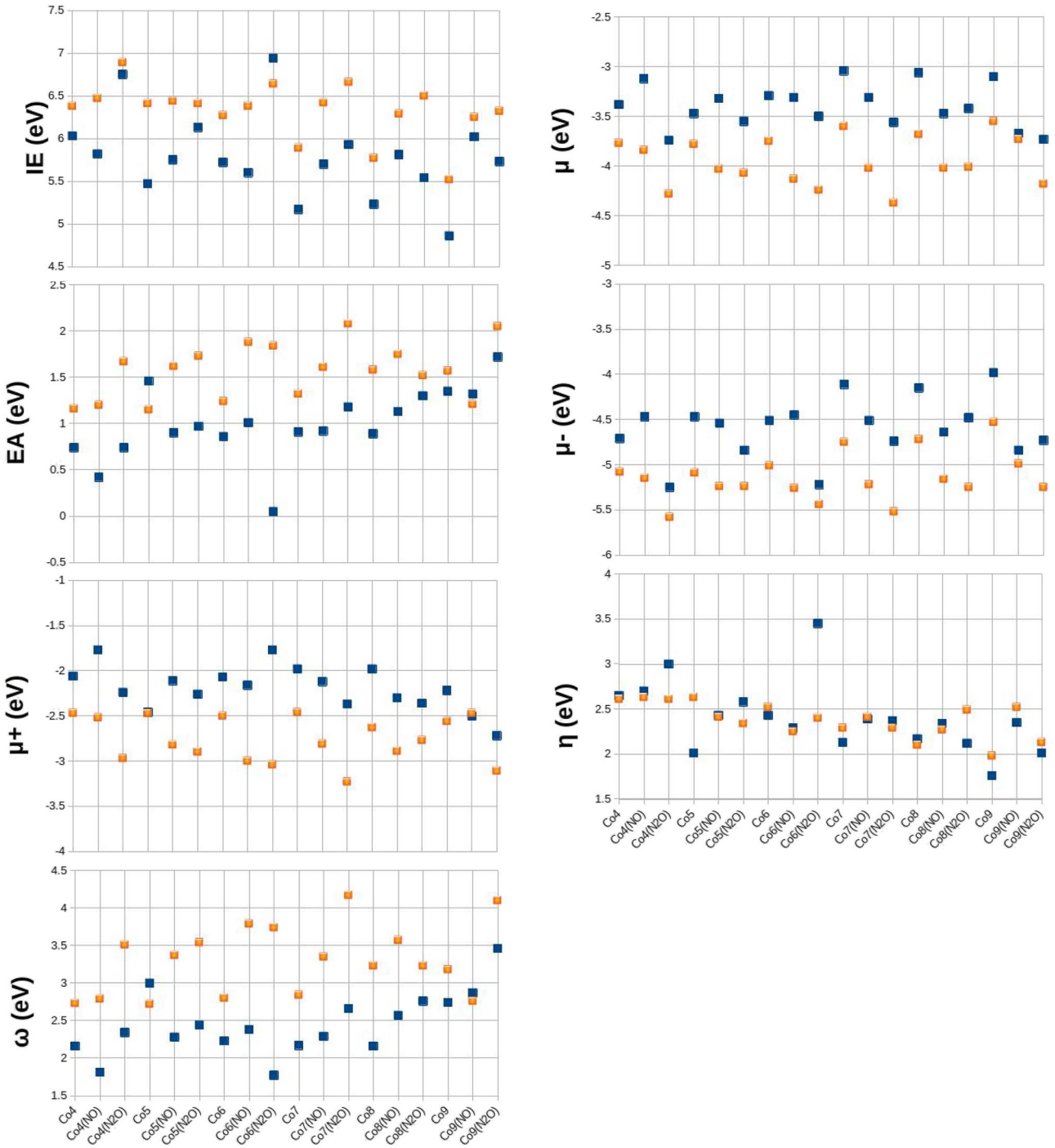

Fig. 7 Ionization energy (*IE*), electron affinity (*EA*), chemical potential (μ), donor chemical potential (μ^-), acceptor chemical potential (μ^+), chemical hardness (η), and electrophilicity index (ω) all in eV. Calculations were performed through *BPW91/6-311G* and *BPW91/6-31G** levels of theory, blue, and orange boxes, respectively

than the other two systems for this size of the cluster, which classifies it as less reactive to losing an electron. In the case of four and six cobalt atoms interacting with N_2O, that is, $Co_4(N_2O)$ and $Co_6(N_2O)$, they have the most considerable ionization potential compared to the other systems studied here, and then, more energy is necessary to remove an electron of these systems.

Concerning the electron affinity, structures Co_4 and $Co_4(N_2O)$ show the same value of this descriptor (6-311G basis set). Therefore, it does not affect the inclusion of the

oxide in Co_4. The calculations made with the basis set without polarization indicate that Co_5 has the highest *EA* compared with $Co_5(NO)$ and $Co_5(N_2O)$, indicating less stability for the addition of an electron. However, by using the 6-31G* basis set, an increase is observed for this descriptor when the pure cluster interacts with *NO* and N_2O. Analysis carried out using 6-311G suggests that for six cobalt atoms, $Co_6(N_2O)$ has the minor *EA* suggesting that it is more stable with electron addition in comparison with the naked structure or containing *NO*. On the other hand, 6-31G* offers an entirely different value for the electronic affinity of $Co_6(N_2O)$, suggesting a behavior almost opposite to that described by the polarized basis set. The *EA* shows no variation between Co_7 and $Co_7(NO)$ systems, this indicates a poor effect of inclusion of *NO* on the surface of Co_7. However, this reactivity slightly increases when Co_7 interacts with N_2O, and then more energy is removed when the system accepts an electron. This behavior is observed for calculations performed with both basis sets. $Co_8(N_2O)$ shows a higher value for the *EA* of the compounds with eight Co atoms, suggesting that it is a system with greater reactivity when gaining an electron (blue boxes); however, it is the system with the lowest value for this reactivity index when calculations are made using 6-31G*, showing a high impact of polarization for this descriptor. Regarding the reactivity to gain an electron (*EA*), there is a small difference in the values found for both Co_9 and $Co_9(NO)$ (see Fig. 7). The *EA* is relatively higher for $Co_9(N_2O)$; consequently, this system shows more tendency to gain an electron. Interestingly, this behavior for these three systems with nine *Co* atoms is the same for the calculations developed using the two base sets, being even lower for $Co_9(NO)$ with 6-31G*.

In the analysis of the results obtained with BPW91/6-311G, it is observed that, about the chemical potential, $Co_4(NO)$ and $Co_5(NO)$ present the highest value suggesting these clusters as the most susceptible to transfer electrons in their respective system sizes. The same applies to Co_6, compared with the interaction with nitric and nitrous oxide.

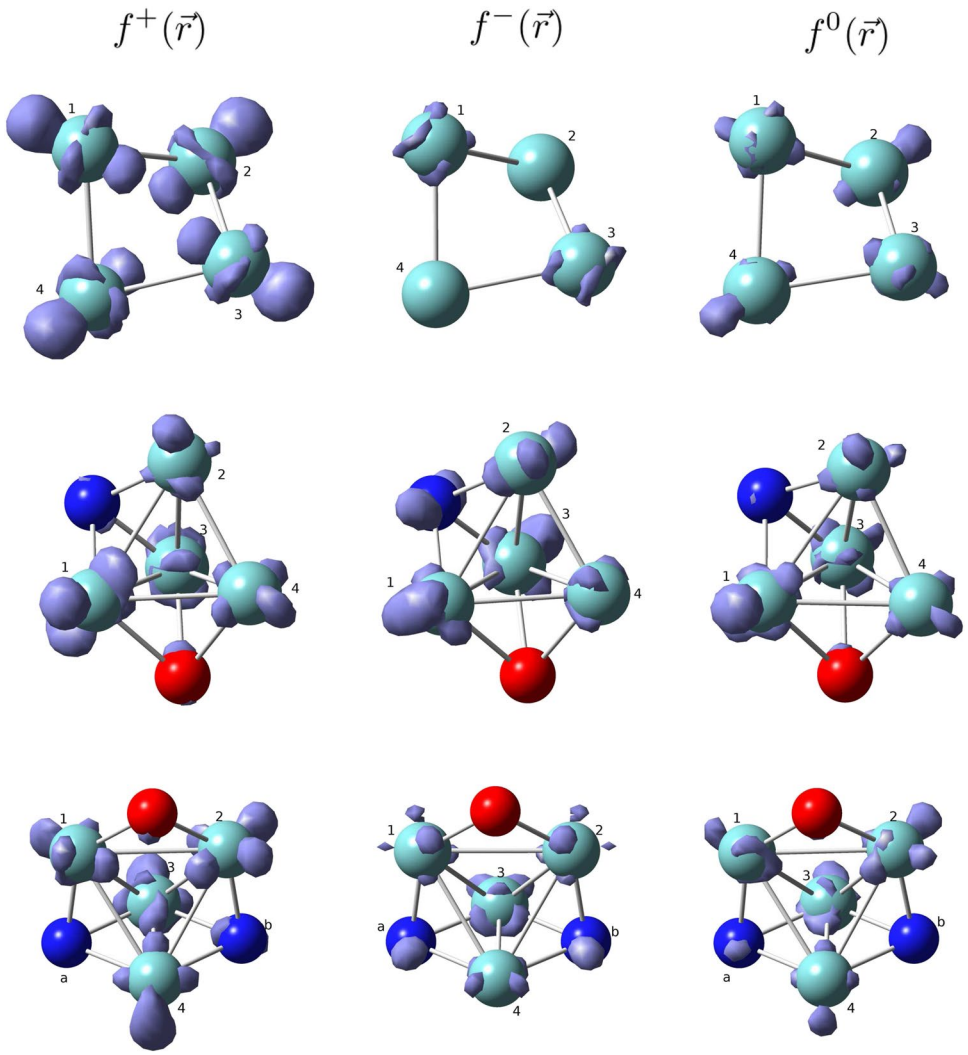

Fig. 8 Fukui functions obtained for Co_4, $Co_4(NO)$, and $Co_4(N_2O)$. Cobalt atoms are shown in blue green, nitrogen atoms in blue, and oxygen atoms in red. The purple regions define the reactivity towards nucleophilic attacks (f^+), electrophilic attacks (f^-), and radical attacks (f^0). Calculations were performed through *BPW91/6-311G* level of theory

For the clusters with four and six cobalt atoms interacting with *NO*, μ^- indicates that these systems can give charge. Conversely, for the cluster with five cobalt atoms, the naked one is more liable to transfer electrons. On the other hand, $Co_4(NO)$ and $Co_5(NO)$ are more liable to accept charge since they have the highest values of μ^+ compared to naked clusters or when N_2O is added. However, $Co_6(N_2O)$ is more prone to accept charge than Co_6 and $Co_6(NO)$. The values for the chemical potential of Co_7, $Co_7(NO)$, and $Co_7(N_2O)$ showed the system becomes less reactive, given the interaction with *NO* and N_2O. Specifically, the results indicate that $Co_7(N_2O)$ has less tendency to exchange electrons. This fact agrees with the values for μ^- and μ^+ of Co_7, since it is the one that shows the highest values for these descriptors, indicating therefore the most reactive compound. From μ values of the clusters with eight Co atoms, it can be concluded that there is a greater tendency of Co_8 to react with other substances because it presents the highest value for this reactivity index. The result for eight Co atoms is very similar to Co_7, that is, Co_8 is the system with the most remarkable tendency both to donate (μ^-) and to accept (μ^+) electrons. Finally, the cluster of nine cobalt atoms becomes less reactive when interacting with N_2O than when it is pure or interacting with *NO* according to the energy difference observed in Fig. 7. Newly, Co_9 shows the highest values of (μ^-) and (μ^+), suggesting it as the most reactive for this number of Co atoms. When comparing the results described above with the values obtained when using the polarized functions for μ, μ^-, and μ^+, it is observed in the respective graphs that the effect of the polarization on these reactivity indices shows a trend where the pure state clusters have the highest values, except for $Co_9(NO)$, which offers the highest value for μ^+.

As the chemical hardness (η) measures the stability of a molecule, that is, the resistance to charge transfer of the system, naked clusters with an even number of cobalt atoms should be the most stable. The results indicate that most of the systems follow the same trend, showing little difference for the calculations made with both basis sets. In the analysis carried out with 6-311G, interestingly, the cluster with five cobalt atoms shows a lower value compared with $Co_5(NO)$ and $Co_5(N_2O)$. The latter indicates a particular reactivity when the cobalt number is odd. Generally, according to Fig. 7, Co_9 is the system with the lowest

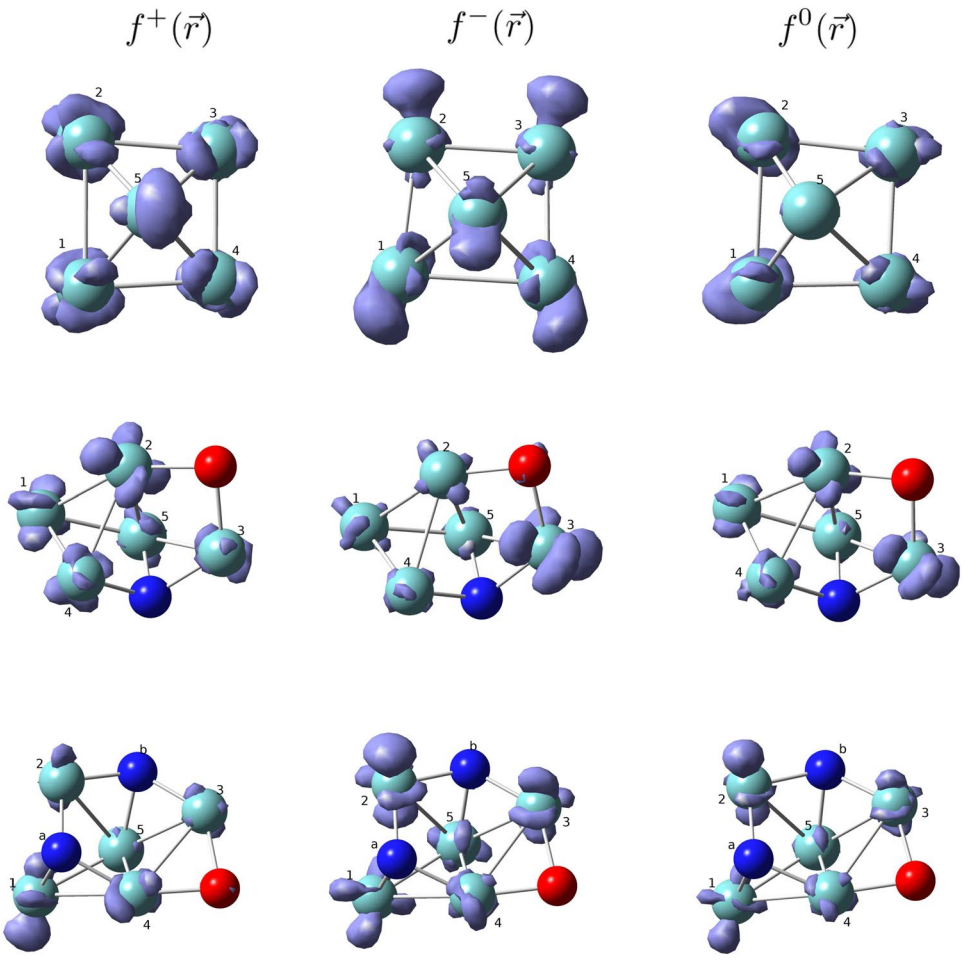

Fig. 9 Fukui functions obtained for Co_5, $Co_5(NO)$, and $Co_5(N_2O)$. Cobalt atoms are shown in blue green, nitrogen atoms in blue, and oxygen atoms in red. The purple regions define the reactivity towards nucleophilic (f^+), electrophilic (f^-), and radical attacks (f^0). Calculations were performed through *BPW91/6-311G* level of theory

η, suggesting the lowest stability of all the systems studied in this work. On the contrary, the $Co_6(N_2O)$ was the most stable structure, presenting the highest hardness value of the clusters studied. In this way, it is possible to observe that the results obtained with this basis set present a more significant variation between systems of different composition, contrary to the results obtained when performing the calculations using the 6-31G* since it seems to tend to a value.

Finally, Fig. 7 shows the electrophilicity index (ω). ω is used to measure the energy stabilization when the system acquires additional electron charge coming from the surroundings; that is, it measures the tendency of chemical species to receive electrons. The blue boxes, which indicate the results for calculations with 6-311G, show that electrophilicity index increases for Co_4 upon the interaction with N_2O and Co_6 when interacting with NO (in comparison with naked clusters, respectively). As this index gives information that can be useful to compare two molecules as an electrophile (which is indicated by a higher ω), it is evident that modified clusters are affected by electron-withdrawing groups reflecting the highest values for ω such as that which happens for the clusters with 7, 8, and 9 cobalt atoms when interacting with NO and N_2O. However, for five cobalt atoms, this index decreases upon the interaction with NO and N_2O. When comparing the results of the calculations carried out with both basis sets, it is observed that this system of five atoms of Co together with $Co_9(NO)$ presents lower values for ω when using the polarized basis function, with the other systems showing higher values when calculations are performed with the 6-31G* basis.

Local reactivity indexes

Figures 8, 9, 10, 11, 12, and 13 show the Fukui functions of the neutral clusters under the theory level BPW91/6-311G. The purple regions on each atom of the respective cobalt cluster define the regions reactive towards nucleophilic attacks (f^+), electrophilic attacks (f^-), and free radicals (f^0).

In Co_4 cluster, it is evident that the four atoms are equally able to receive a nucleophilic attack, but not for an electrophilic attack, where atoms **1** and **3** are the most

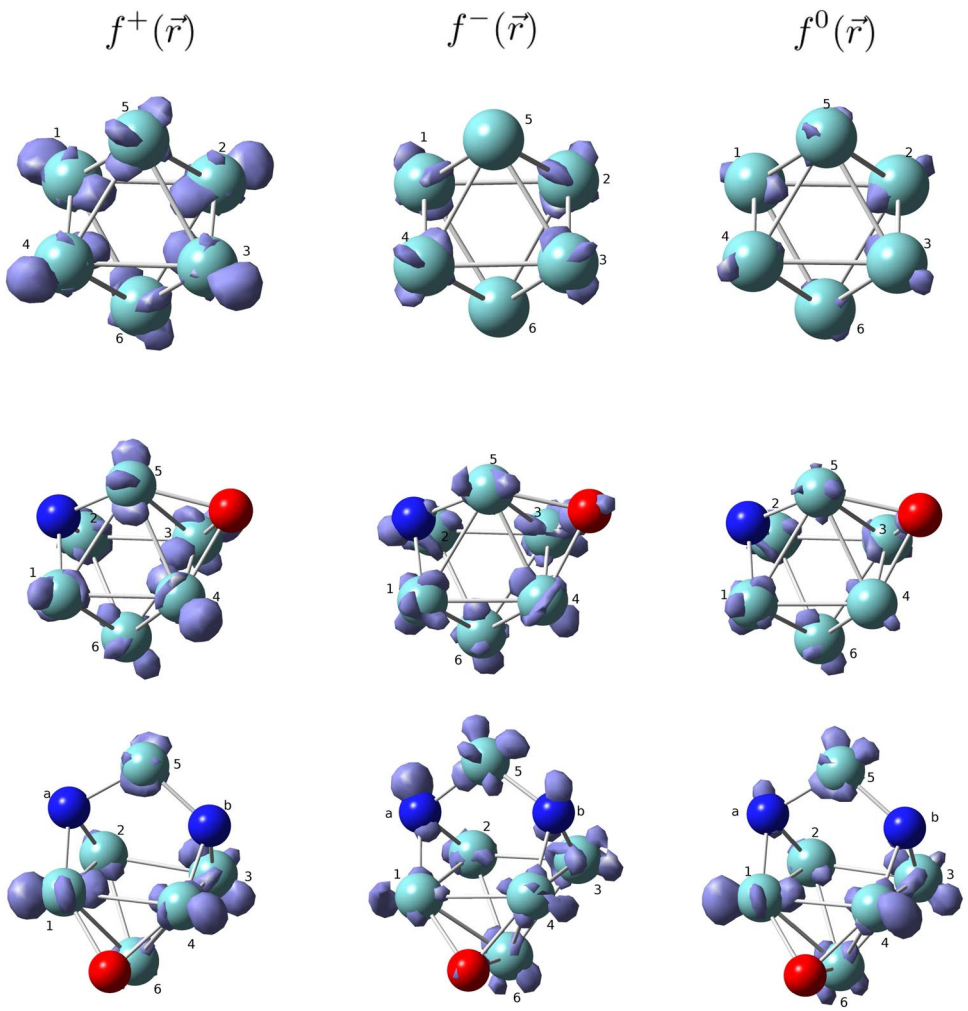

Fig. 10 Fukui functions obtained for Co_6, $Co_6(NO)$, and $Co_6(N_2O)$. Cobalt atoms are shown in blue green, nitrogen atoms in blue, and oxygen atoms in red. The purple regions define the reactivity towards nucleophilic (f^+), electrophilic (f^-), and radical attacks (f^0). Calculations were performed through *BPW91/6-311G* level of theory

susceptible to be electrophilically attacked. Because of the asymmetry between f^+ and f^-, f^0 shows atoms **2** and **4** as the most probable sites to receive radical attacks as is expected since f^0 is an average of f^+ and f^- indexes. For $Co_4(NO)$ cluster, cobalt atom labeled as **1**, which is between nitrogen and oxygen atoms, is the ablest to have a nucleophilic attack. Cobalt **1** and **3** are susceptible to electrophilic and radical attacks. Regarding the $Co_4(N_2O)$ cluster, the cobalt atoms present the same probability of receiving a nucleophilic reaction. Moreover, nitrogen atoms could also be susceptible to presenting an electrophilic attack, in virtue of the f^- Fukui function. Finally, reaction to a radical could be performed mainly in cobalt **2** and **4**.

About systems with five cobalt atoms, the geometry of Co_5 seems essential in its reactivity (see Fig. 9). The distances from cobalt atoms **1** and **2** to number **5** are more prominent than the distance from cobalt atoms **3** and **4** to cobalt **5**. This apparent reduction of symmetry is likely the reason for the fact that f^+ Fukui function is the same in atoms **1** and **2** or atoms **3** and **4**. However, when the *NO* molecule interacts with the cluster, it breaks the symmetry resulting in cobalt **2** as the most reactive to this attack. Additionally, N_2O induces a strong reactivity in cobalt atoms **1** and **4**. Concerning the electrophilic attack, Fig. 9 shows a similar reactivity in all cobalt atoms of Co_5 cluster, atom **5** being the one with slight differences with the other atoms. The electrophilic attack to $Co_5(NO)$ occurs most likely in the proximity to *O* and *N*; that is, atom **3** is the most susceptible to give electrons. It is also evident that the most significant electrophilic reactivity for the cluster $Co_5(N_2O)$ is located in the cobalt atom **1** and **2**, far away from the oxygen atom. On the other hand, atoms **1** and **2** have a considerable f^0 Fukui function in the pure cluster. In the case of the system $Co_5(NO)$, it is evident that cobalt **3** is the most probable atom for receiving a radical attack. Besides, it is worth to note the most proximate atoms to oxygen are the most reactive to radicals. Thus, atoms **1** and **2** are also the most reactive sites to radicals in $Co_5(N_2O)$ system.

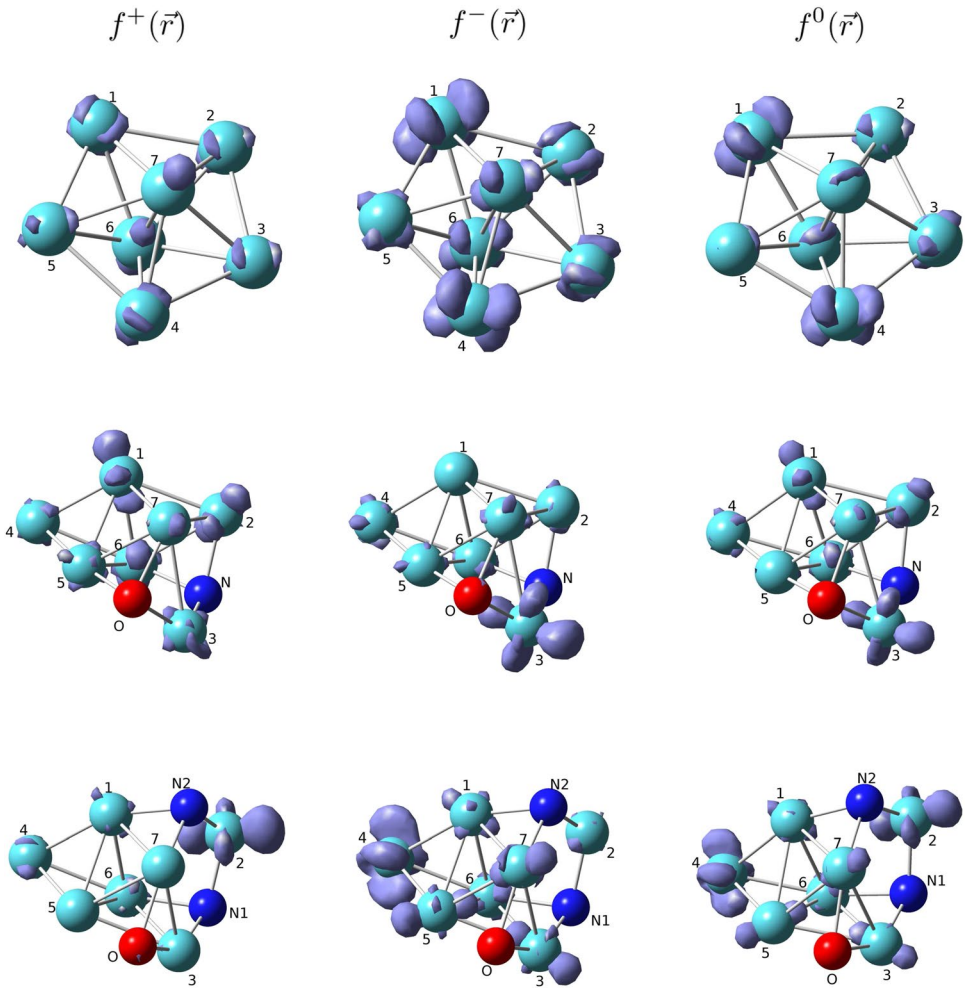

Fig. 11 Fukui functions obtained for Co_7, $Co_7(NO)$, and $Co_7(N_2O)$. Cobalt atoms are shown in blue green, nitrogen atoms in blue, and oxygen atoms in red. The purple regions define the reactivity towards nucleophilic (f^+), electrophilic (f^-), and radical attacks (f^0). Calculations were performed through *BPW91/6-311G* level of theory

Fukui functions in Fig. 10 for Co_6 show reactivity towards nucleophilic attacks centered mainly on the atoms that are the base of the square bipyramid, that is, numbers **1** to **4**. On the other hand, atoms **5** and **6** also show reactivity but at a lower level. In the case of the $Co_6(NO)$ system, it is clear that nucleophilic reactivity is more significant in atoms **3** and **4**, indicating that the oxygen atom plays an essential role in redistributing densities in the cluster with six cobalt atoms. Concerning the nucleophilic attack at $Co_6(N_2O)$ system, atoms **1**, **3**, and **4** show the most reactive sites. Regarding the electrophilic attack, Co_6 cluster exhibits a negligible reactivity in the sites located at the base of the bipyramid, suggesting that the electron density available to give electrons is sparse. In the $Co_6(NO)$ system, atoms forming the base of the bipyramid present the most considerable f^-; however, nitrogen and oxygen atoms also have this Fukui function. In the case of $Co_6(N_2O)$, all cobalt atoms and both nitrogen atoms are susceptible to give electrons. For radical attacks, the naked cluster has almost no f^0 Fukui function. For $Co_6(NO)$, atoms **1**, **2**, and **6** present a small contribution of the Fukui function; moreover, cobalt atoms closer to oxygen have the lowest reactivity toward radical attacks. Finally, atoms **1**, **3**, and **4** of cobalt in $Co_6(N_2O)$ have the most significant amount of f^0, indicating these sites as the most probable to receive a radical attack.

The local reactivity calculated by Fukui functions for Co_7 shows areas with higher nucleophilic probability; this reactivity is on the atoms **6** and **7** corresponding to the atoms that form the axis of the pentagonal bipyramid. Furthermore and according to Fig. 11, all atoms of the system are susceptible to gaining charge density (f^+). On the other side, atoms **1** and **4** show a more considerable affinity to electrophilic attacks. In addition, these atoms concentrate a higher reactive proportion toward a radical attack. The $Co_7(NO)$ composition shows that the regions with nucleophilic susceptibility are in cobalt atoms **1**, **2**, and **6**. These atoms are further away from the oxygen atom (see Fig. 11). In the same table, cobalt atom **3** has the most electrophilic area in this cluster, thus indicating the region with the highest charge concentration. Reactivity toward radical attacks also focuses on the cobalt atom **3**, where the largest reactivity area is exhibited. For

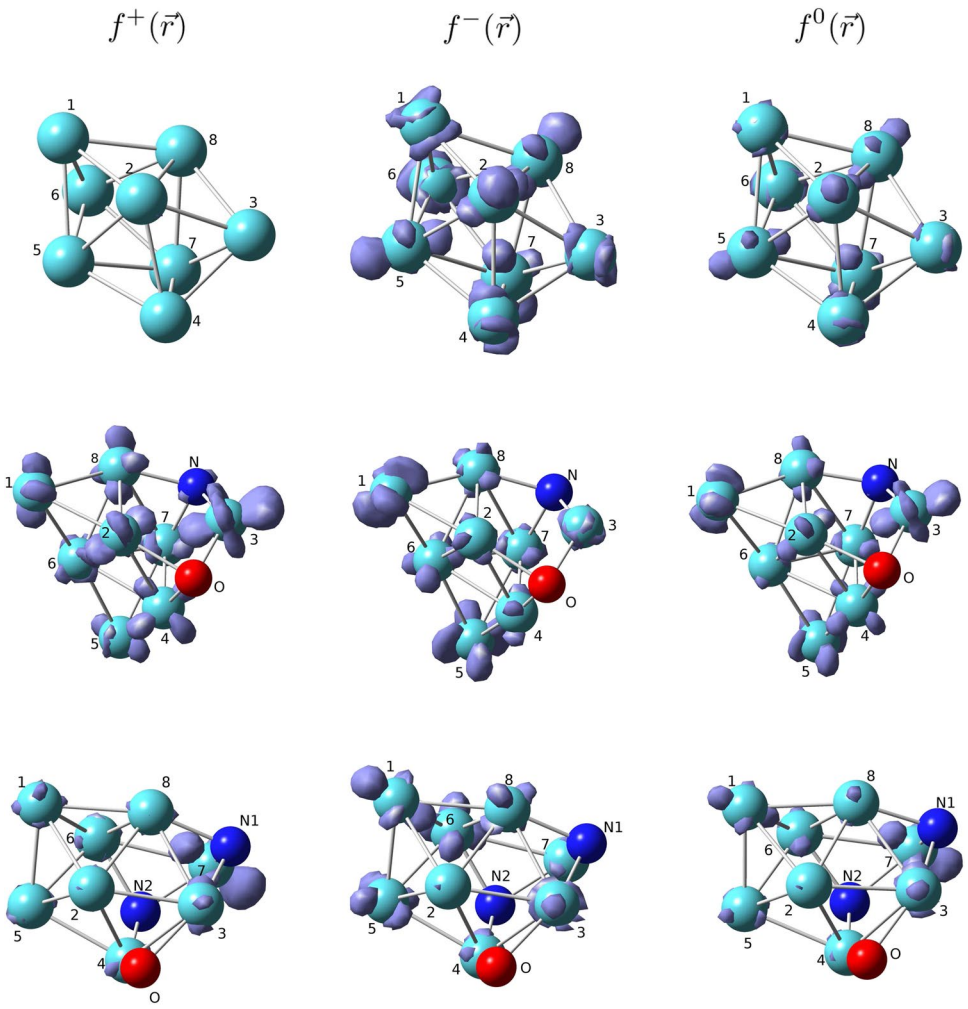

Fig. 12 Fukui functions obtained for Co_8, $Co_8(NO)$, and $Co_8(N_2O)$. Cobalt atoms are shown in blue green, nitrogen atoms in blue, and oxygen atoms in red. The purple regions define the reactivity towards nucleophilic (f^+), electrophilic (f^-), and radical attacks (f^0). Calculations were performed through *BPW91/6-311G* level of theory

$Co_7(N_2O)$ composition, the *Co* atom **2** has the area most likely to gain electrons. This atom is between the two nitrogen atoms; and therefore, this reactivity could be dictated by them. The electrophilic reactivity on $Co_7(N_2O)$ is on the cobalt atoms **4** and **6**, which are far away from the oxygen atom. Figure 11 shows that the reactivity toward radicals is most likely in atoms **2** and **4** of cobalt and lesser amounts for cobalt atom **3**.

The Co_8 system shows no significant reactivity toward nucleophilic attacks, according to Fig. 12. However, for the electrophilic attack, this system has susceptible areas in all cobalt atoms. The regions that most likely react toward attacks with radical species are on atoms **5** and **8**. The $Co_8(NO)$ composition shows that the nucleophilic attack could be more likely in atoms **1**, **3**, and **8**. Electrophilic zones are present on atoms **1**, **5**, and **6**, further away from the atoms of *O*. The highest reactivity toward radicals on $Co_8(NO)$ system is on cobalt atoms **1**, **3**, and **5**. The $Co_8(N_2O)$ composition shown in Fig. 12 indicates that the nucleophilic activity is on the cobalt atoms **3** and **7**; interestingly, these atoms have closer proximity to the pair of *N* atoms. The electrophilic reactivity for the same system is on distant regions to the zone where the nitrogen atoms have been chemisorbed, that is, on cobalt atoms **1** and **6**. The average of the two reactivity indexes discussed above has higher intensity on atoms **1**, **3**, and **6**.

Figure 13 shows for Co_9 that the area with the most possibility to receive nucleophilic and electrophilic attacks is on atoms **1**, **3**, **4**, and **6**, which are at the vertices of this hexagonal structure. Nonetheless, atoms **2** and **5** have equivalent regions that are susceptible to these reactivities. Additionally, the nine atoms of the *Co* cluster should not be reactive toward radicals since the surface does not show susceptible areas. Fukui functions for the $Co_9(NO)$ system can also be observed in Fig. 13; it is clear that the susceptible regions toward nucleophilic attack are present in all cobalt atoms, being in the smaller amount on atoms that are close to the oxygen atom. For f^-, it is shown that the atoms **2**, **4**, **8**, and **9** are more likely to lose charge density. Finally, for reactivity towards radicals, all cobalt atoms of $Co_9(NO)$ system show susceptible areas, except atom **3**, which is close to the oxygen atom. Figure 13 further shows the Fukui functions

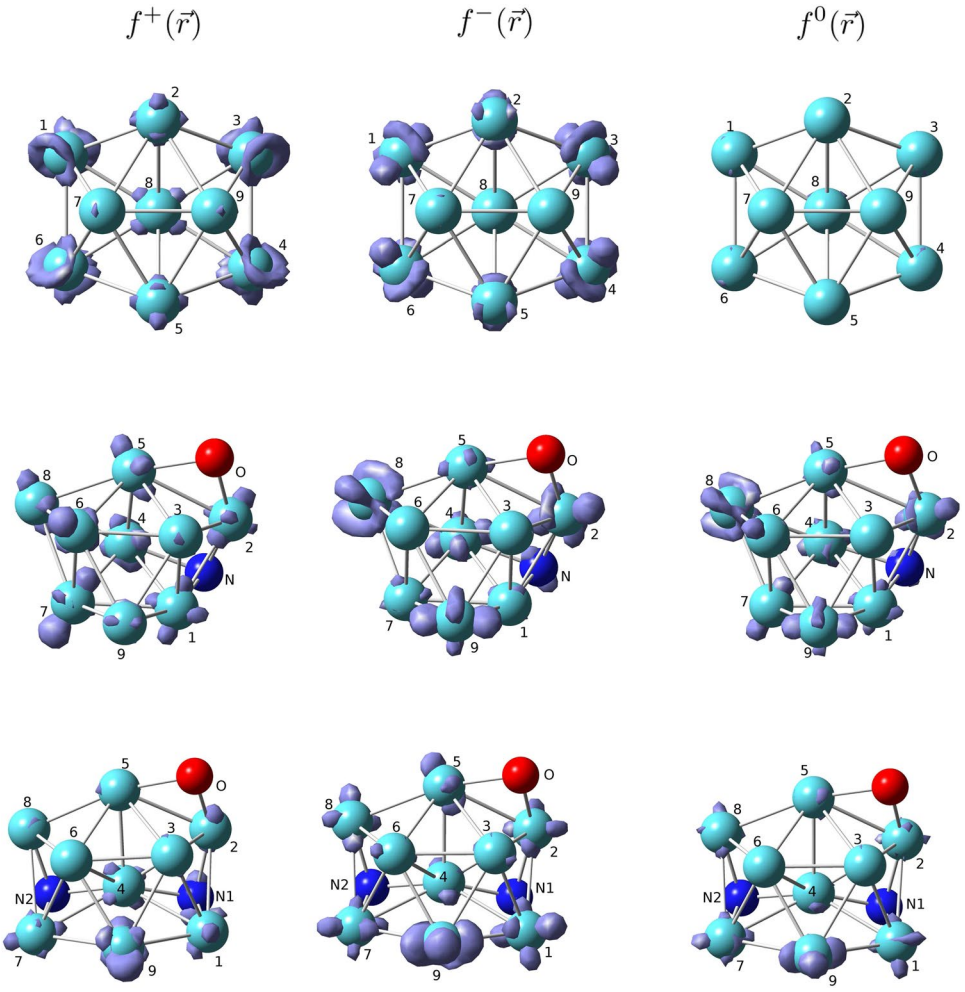

Fig. 13 Fukui functions obtained for Co_9, $Co_9(NO)$, and $Co_9(N_2O)$. Cobalt atoms are shown in blue green, nitrogen atoms in blue, and oxygen atoms in red. The purple regions define the reactivity towards nucleophilic (f^+), electrophilic (f^-), and radical attacks (f^0). Calculations were performed through *BPW91/6-311G* level of theory

for $Co_9(N_2O)$. Atoms **1**, **7**, and **9** show the largest areas susceptible to receive both nucleophilic and electrophilic attacks, being also the most favored for a radical attack.

Binding energies for $Co_n^q(NO)$ and $Co_n^q(N_2O)$ where n=4–9 and q=0–1

For a system, the most negative binding energy is the most energy required to separate the system; and therefore, the system has high stability. In Table 3, it is shown the binding energies (in eV) for the different cluster sizes interacting with *NO* and N_2O. The calculations were developed under the theory levels BPW91/6-311G and BPW91/6-31G*. For all cluster sizes interacting with both nitrous oxides, the binding energies are negatives, suggesting that clusters with nitrous oxides are more stable than Co^q, *N*, and *O* separated atoms. In general, neutral systems showed larger E_b's than cation systems, which imply less stability. In addition, for these neutral systems, an even-odd behavior is observed, where systems with an odd number of *Co* atoms exhibit more negative E_b's, indicating more stability compared to those with an even number of *Co* atoms. For cation systems, the E_b's are lower with the increasing number of *Co* atoms, suggesting the dependence of stability on the size of the cluster, and hence the high probability of formation of the systems studied here. It is worth mentioning that this is observed in the experimental literature [15, 18].

Summary and conclusions

Molecular dissociation of nitric oxide and nitrous oxide is one of the crucial tasks that would help reduce and prevent environmental problems, and cobalt clusters show an essential contribution due to their catalytic activity. From these results, the dissociative chemisorption of *NO* and N_2O on small cobalt clusters is evident, and no cluster fragmentation occurs, which is in line with reported data. The present study shows an alternative for obtaining information on these clusters and, in this way, makes possible the design of catalysts that involve the segmentation of these molecules. Also, according to the results obtained in this work, it is suggested that the methodology used is adequate for searching minimums on the potential energy surface. Due to the remarkable similarity between the pure systems and the reported geometries in the literature, that is, since the geometries found for the clusters with 4, 5, 6, 7, 8, and 9 *Co* atoms are in good agreement with other works, it inspires confidence that the methodology followed here is adequate and affirms that the rest of the structures correspond to a minimum. In this way, one can suggest that cobalt clusters act dissociating *NO* and N_2O molecules.

Interestingly, global reactivity indexes show an even-odd effect. *IE* is one of the physical properties that are currently amenable to experimental measurement. Also, their dependence on cluster size provides information about the electronic behavior of these species. According to the results with BPW91/6-311G, it is observed that cobalt clusters with an even number of atoms show an increase in *IE* descriptor as the cluster interacts with N_2O and decreases when it interacts with *NO*. For 7, 8, and 9 cobalt atoms, the clusters showed the lowest *IE* compared with the species containing *NO* and N_2O. Concerning the *IE* results with BPW91/6-31G*, except for the clusters with five *Co* atoms, in all other systems, ionization potential increases when comparing the cluster pure with the interaction with *NO* and N_2O. *EA* also suggested an even-odd behavior for the naked structures, where clusters with an odd number of cobalt atoms have higher electron affinity values. About the chemical potential, for all system sizes, except Co_8, this descriptor suggests less reactivity when the clusters are interacting with N_2O. In this sense, these systems present more negative values of μ. This fact agrees with the μ^- values except for the Co_8 and

Table 3 Binding energy (E_b) for $Co_n^q(NO)$ and $Co_n^q(N_2O)$ (n = 4–9 and q = 0,1)

System	E_b (*BPW91/6-311G*)	E_b (*BPW91/6-31G**)
$Co_4(NO)$	−20.92	−24.38
$Co_4^+(NO)$	−142.24	−48.48
$Co_4(N_2O)$	−26.92	−30.83
$Co_4^+(N_2O)$	−147.15	−53.66
$Co_5(NO)$	−24.74	−28.87
$Co_5^+(NO)$	−177.83	−60.76
$Co_5(N_2O)$	−30.99	−35.11
$Co_5^+(N_2O)$	−182.72	−66.83
$Co_6(NO)$	−28.47	−34.03
$Co_6^+(NO)$	−213.62	−73.14
$Co_6(N_2O)$	−35.21	−40.66
$Co_6^+(N_2O)$	−219.97	−80.05
$Co_7(NO)$	−32.60	−38.85
$Co_7^+(NO)$	−249.43	−86.08
$Co_7(N_2O)$	−39.47	−45.61
$Co_7^+(N_2O)$	−255.81	−92.26
$Co_8(NO)$	−36.75	−43.75
$Co_8^+(NO)$	−284.86	−98.62
$Co_8(N_2O)$	−43.12	−50.11
$Co_8^+(N_2O)$	−291.13	−104.86
$Co_9(NO)$	−40.56	−49.04
$Co_9^+(NO)$	−320.96	−111.52
$Co_9(N_2O)$	−45.80	−54.78
$Co_9^+(N_2O)$	−326.39	−117.14

Calculations were performed by *BPW91/6-311G* and *BPW91/6-31G** levels of theory. Energy in eV

Co_9 sizes, where the clusters with the slightest tendency to transfer electrons are when the Co_8 and Co_9 systems interact with NO. Co_7, Co_8, and Co_9, shows the highest values for μ^- and μ^+, indicating, therefore, that they are more reactive than when they interact with NO or N_2O. The chemical hardness values also show an even-odd behavior for the naked structures. Co_9 is the system with the lowest resistance to charge transfer, suggesting the lowest stability of all the systems studied here. Finally, under the level of theory BPW91/6-311G, the clusters with 7, 8, and 9 cobalt atoms have a better tendency to stabilize an electron acquired from their environment when interacting with NO and N_2O, due to the highest values of ω.

Through the Fukui function, it is possible to predict the local reactivity of the systems. For all the studied systems in this work, nucleophilic, electrophilic, and radical sites were investigated to predict the next possible site to attack on each system.

We believe that the results presented here may be valuable for a better understanding of Co clusters, their reactivity, and their use in dissociating toxic environmental molecules such as NO and N_2O.

Supplementary Information The online version contains supplementary material available at https://doi.org/10.1007/s00894-022-05165-0.

Acknowledgements JGFM acknowledges the National Council of Science and Technology (CONACYT) for the doctoral fellowship with number 502772. The authors also acknowledge the University of Guadalajara for financial support. The authors would like to acknowledge the computational resources and technical support offered by the Data Analysis and Supercomputing Center (CADS, for its acronym in Spanish) of the University of Guadalajara through *Leo Atrox* supercomputer.

Author Contributions JGFM performed research, wrote the manuscript, and analyzed data. DAHV assisted with figures and analyzed data. GRG analyzed data. RFM reviewed the manuscript. JGRZ reviewed the manuscript, analyzed data, and assisted with figures and tables. FJTR designed research, wrote the manuscript, and analyzed data.

Funding JGFM received from the National Council of Science and Technology (CONACYT) the doctoral fellowship with number 502772. The authors also received financial support from the University of Guadalajara.

Availability of data and material The raw data required to reproduce these findings cannot be shared at this time due to technical or time limitations. They can be obtained via email to the corresponding author. However, final structures and energies are included as supplementary material.

Code availability Not applicable

Supplementary information Authors reporting cartesian coordinates and energies for all optimized geometries of Co_n^q, $Co_n^q(NO)$, and $Co_n^q(N_2O)$ ($q = 0, 1$ and $n = 4 - 9$).

Declarations

Conflict of interest The authors declare no competing interests.

References

1. Stocker TF, Qin D, Plattner G-K, Tignor MMB, Allen SK, Boschung J, Nauels A, Xia Y, Bex V, Midgley PM (2013) IPCC, 2013: Climate change 2013: The physical science basis. Contribution of working group I to the fifth assessment report of the intergovernmental panel on climate change. Cambridge University Press, Cambridge, United Kingdom, and New York, NY (USA)
2. Mussati DC, Srivastava R, Hemmer PM, Strait R, Pechan EH (2000) Section 4. NO_x Controls. Section 4.2NO_x Post-combustion selective catalytic reduction contents. U. S. Environmental Protection Agency, 2–59. https://doi.org/EPA/452/B-02-001
3. Sorrels JL, Randall DD, Schaffner KS, Fry CR (2016). Selective catalytic reduction. EPA Air pollution control cost manual. **U.S. Environmental Protection Agency**. https://www3.epa.gov/ttn/ecas/docs/SCRCostManualchapter7thEdition_2016.pd
4. Piskorz W, Zasada F, Stelmachowski P, Kotarba A, Sojka Z (2008) Descomposition of N_2O over surface of cobalt spinel: A dft account of reactivity experiments. Catalysis Today 137(2):418–422. https://doi.org/10.1016/j.cattod.2008.02.027
5. Kondow T, Mafuné F (2003) Experimental and theoretical studies of clusters. World Scientific Publishing Co. Pte. Ltd, USA
6. Kawazoe Y, Kondow T, Ohno K (2002) Clusters and nanomaterials. Theory and experiment. Springer, USA
7. Knickelbein MB (1999) Reactions of transition metal clusters with small molecules. Annual Review of Physical Chemistry 50(1):79–115. https://doi.org/10.1146/annurev.physchem.50.1.79
8. March NH (1986) Chemical bonds outside metal surfaces. Plenum: New York. Boston, MA : Springer US, NY (USA)
9. Blanchet C, Duarte HA, Salahub DR (1997) Density functional study of mononitrosyls of first-row transition-metal atoms. The Journal of Chemical Physics 106(21):8778–8787. https://doi.org/10.1063/1.473938
10. Ford MS, Anderson ML, Barrow MP, Woodruff DP, Drewello T, Derrick PJ, Mackenzie SR (2005) Reactions of nitric oxide on Rh_6^+ clusters: abundant chemistry and evidence of structural isomers. Physical Chemistry Chemical Physics 7(5):975–980. https://doi.org/10.1039/B415414B
11. Rodríguez-Kessler PL, Rodríguez-Domínguez AR (2015) N_2O dissociation on small Rh clusters: A density functional study. Computational Materials Science 97(c):32–35. https://doi.org/10.1016/j.commatsci.2014.09.044
12. Rodríguez-Kessler PL, Pan S, Florez E, Cabellos JL, Merino G (2017) Structural evolution of the rhodium-doped silver clusters Ag_nRh ($n \leq 15$) and their reactivity toward NO. The Journal of Physical Chemistry C 121(35):19420–19427. https://doi.org/10.1021/acs.jpcc.7b05048
13. Klaassen JJ, Jacobson DB (1988) Dissociative versus molecular chemisorption of nitric oxide on small bare cationic cobalt clusters in the gas phase. Journal of the American Chemical Society 110(3):974–976. https://doi.org/10.1021/ja00211a052
14. Klaassen JJ, Jacobson DB (1989) Facile oxygen exchange by cobalt cluster oxide ions with water-oxygen-18 in gas phase. Inorganic Chemistry 28(11):2022–2024. https://doi.org/10.1021/ic00310a003
15. Anderson ML, Lacz A, Drewello T, Derrick PJ, Woodruff DP, Mackenzie SR (2009) The chemistry of nitrogen oxides on small size-selected cobalt clusters Co_n^+. The Journal of Chemical Physics 130(6):064305. https://doi.org/10.1063/1.3075583

16. Martínez A, Jamorski C, Medina G, Salahub DR (1998) Molecular versus dissociative chemisorption of nitric oxide on Co_2 and Co_3 (neutral and cationic). A density functional study. The Journal of Physical Chemistry A 102(24):4643–4651. https://doi.org/10.1021/jp980393c
17. Hanmura T, Ichihashi M, Okawa R, Kondow T (2009) Size-dependent reactivity of cobalt cluster ions with nitrogen monoxide: Competititon between chemisorption and descomposition of *NO*. International Journal of Mass Spectrometry 280(1):184–189. https://doi.org/10.1016/j.ijms.2008.08.024
18. Koyama K, Kudoh S, Miyajima K, Mafuné F (2015) Thermal desorption spectroscopy study of the adsorption and reduction of *NO* by cobalt cluster ions under thermal equilibrium conditions at 300 k. The Journal of Physical Chemistry A 119(37):9573–9580. https://doi.org/10.1021/acs.jpca.5b05320
19. Alexandrova AN, Boldyrev AI (2005) Search for the $Li_n^{0/+1/-1}$ (n = 5–7). Lowest-energy structures using the *ab initio* Gradient Embedded Genetic Algorithm (GEGA). Elucidation of the chemical bonding in the lithium clusters. Journal of Chemical Theory and Computation 1(4):566–580. https://doi.org/10.1021/ct050093g
20. Vosko SH, Wilk L, Nusair M (1980) Accurate spin-dependent electron liquid correlation energies for local spin density calculations: a critical analysis. Canadian Journal of Physics 58(8):1200–1211. https://doi.org/10.1139/p80-159
21. Hay PJ, Wadt WR (1985) *Ab initio* effective core potentials for molecular calculations. Potentials for the transition metal atoms *Sc* to *Hg*. The Journal of Chemical Physics 82(1):270–283. https://doi.org/10.1063/1.448799
22. Dunning Jr, TH, J, HP (1977) In modern theoretical chemistry. Ed. H. F. Schaefer III, (Plenum, New York, 1-28)
23. Guzmán-Ramírez G, Robles J, Vega A, Aguilera-Granja F (2011) Stability, structural, and magnetic phase diagrams of ternary ferromagnetic 3d-transition-metal clusters with five and six atoms. The Journal of Chemical Physics 134(5):054101. https://doi.org/10.1063/1.3533954
24. Frisch MJ, Trucks GW, Schlegel HB, Scuseria GE, Robb MA, Cheeseman JR, Scalmani G, Barone V, Mennucci B, Petersson GA, Nakatsuji H, Caricato M, Li X, Hratchian HP, Izmaylov AF, Bloino J, Zheng G, Sonnenberg JL, Hada M, Ehara M, Toyota K, Fukuda R, Hasegawa J, Ishida M, Nakajima T, O Kitao YH, Nakai H, Vreven T, Montgomery JA Jr, Peralta JE, Ogliaro F, Bearpark M, Heyd JJ, Rothers EB, Kudin KN, Staroverov VN, Kobayashi R, Normand J, Raghavachari K, Rendell A, Burant JC, Yengar SSI, Tomasi J, Cossi M, Rega N, Millam JM, Klene M, Knox JE, Cross JB, Bakken V, Adamo C, Jaramillo J, Gomperts R, Stratmann RE, Yazyev O, Austin AJ, Cammi R, Pomelli C, Ochterski JW, In RLM, Morokuma K, Zakrzewski VG, Voth GA, Salvador P, Dannenberg JJ, Dapprich S, Daniels AD, Farkas, O, Foresman, JB, Ortiz, JV, Cioslowski, J, Fox, DJ (2009) Gaussian09 Revision C01 gaussian Inc Wallingford CT
25. Frisch MJ, Trucks GW, Schlegel HB, Scuseria GE, Robb MA, Cheeseman JR, Scalmani G, Barone V, Petersson GA, Nakatsuji H, Li X, Caricato M, Marenich AV, Bloino J, Janesko BG, Gomperts R, Mennucci B, Hratchian HP, Ortiz JV, Izmaylov AF, Sonnenberg JL, Williams-Young D, Ding F, Lipparini F, Egidi F, Goings J, Peng B, Petrone A, Henderson T, Ranasinghe D, Ski VGZ, Gao J, Rega N, Zheng G, Liang W, Hada M, Ehara M, Toyota K, Fukuda R, Hasegawa J, Shida MI, Nakajima T, Honda Y, Kitao O, Nakai H, Vreven T, Throssell K, Montgomery JA Jr, Peralta JE, Ogliaro F, Bearpark MJ, Heyd JJ, Brothers EN, Kudin KN, Staroverov VN, Keith TA, Kobayashi R, Normand J, Raghavachari K, Rendell AP, Burant JC, Iyengar SS, Tomasi J, Cossi M, Millam JM, Klene M, Adamo C, Cammi R, Ochterski JW, Martin RL, Morokuma K, Farkas O, Foresman JB, Fox DJ (2016) Gaussian16 Revision C01 Gaussian Inc Wallingford CT
26. Becke AD (1988) Density-functional exchange-energy approximation with correct asymptotic behavior. Physical Review A 38(6):3098–3100. https://doi.org/10.1103/PhysRevA.38.3098
27. Perdew JP (1986) Density-functional approximation for the correlation energy of the inhomogeneous electron gas. Physical Review B 33(12):8822–8824. https://doi.org/10.1103/PhysRevB.33.8822
28. Wang Y, Perdew JP (1991) Spin scaling of the electron-gas correlation energy in the high-density limit. Physical Review B 43(11):8911–8916. https://doi.org/10.1103/PhysRevB.43.8911
29. Perdew JP, Wang Y (1992) Accurate and simple analytic representation of the electron-gas correlation energy. Physical Review B 45(23):13244–13249. https://doi.org/10.1103/PhysRevB.45.13244
30. Zhao Y, Schultz NE, Truhlar DG (2005) Exchange-correlation functional with broad accuracy for metallic and nonmetallic compunds, kinetics, and noncovalent interactions. The Journal of Chemical Physics 123(16):161103. https://doi.org/10.1063/1.2126975
31. Zhao Y, Schultz NE, Truhlar DG (2006) Design of density functionals by combining the method of constraint satisfaction with parametrization for thermochemistry, thermochemical kinetics, and noncovalent interactions. Journal of Chemical Theory and Computation 2(2):364–382. https://doi.org/10.1021/ct0502763
32. Zhao Y, Truhlar DG (2008) The M06 suit of density functionals for main group thermochemistry, thermochemical kinetics, noncovalent interaction, excited states, and transition elements: two new functionals and systematic testing of four m06-class functionals and 12 other functionals. Theoretical Chemistry Accounts 120(1–3):215–241. https://doi.org/10.1007/s00214-007-0310-x
33. Zhao Y, Truhlar DG (2006) A new local density functional for main-group thermochemistry, transition metal bonding, thermochemical kinetics, and noncovalent interaction. The Journal of Chemical Physics 125(19):194101. https://doi.org/10.1063/1.2370993
34. Krishnan R, Binkley JS, Seeger R, Pople JA (1980) Self-consistent molecular orbital methods. XX. A basis set for correlated wave functions. The Journal of Chemical Physics 72(1):650–654. https://doi.org/10.1063/1.438955
35. Godbout N, Salahub D, Andzelm J, Wimmer E (1992) Optimization of gaussian-type basis sets for local spin density functional calculations. Part I. Boron through neon, optimization technique and validation. Canadian Journal of Chemistry 70(2):560–571. https://doi.org/10.1139/v92-079
36. Sosa C, Andzelm J, Elkin BC, Wimmer E, Dobbs KD, Dixon DA (1992) A local density functional study of the structure and vibrational frequencies of molecular transition-metal compounds. The Journal of Physical Chemistry 96(16):6630–36. https://doi.org/10.1021/j100195a022
37. Fuentealba P, Preuss H, Stoll H, Szentpály LV (1982) A proper account of core-polarization with pseudopotentials: single valence-electron alkali compounds. Chemical Physics Letters 89(5):418–422. https://doi.org/10.1016/0009-2614(82)80012-2
38. Morse MD (1986) Clusters of transition-metal atoms. Chemical Reviews 86(6):1049–1109. https://doi.org/10.1021/cr00076a005
39. Kant A, Strauss B (1964) Dissociation energies of diatomic molecules of the transition elements. II. Titanium, chromium, manganese, and cobalt. The Journal of Chemical Physics 41(2):3806–3808. https://doi.org/10.1063/1.1725817
40. Gutsev GL, Bauschlicher CW (2003) Electron affinities, ionization energies, and fragmentation energies of Fe_n clusters (n=2-6): A density functional theory study. The Journal of Physical Chemistry A 107(36):7013–7023. https://doi.org/10.1021/jp030288p
41. Rassolov VA, Pople JA, Ratner MA, Windus TL (1998) 6–31g* basis set for atoms *K* through *Zn*. The Journal of Chemical Physics 109(4):1223–1229. https://doi.org/10.1063/1.476673

42. Hariharan PC, Pople JA (1973) The influence of polarization functions on molecular orbital hydrogenation energies. Theoretica Chimica Acta 28(3):213–222. https://doi.org/10.1007/BF00533485
43. Parr RG, Weitao Y (1994) Density-functional theory of atoms and molecules. Oxford University Press, USA
44. Parr RG, Donnelly RA, Levy M, Palke WE (1978) Electronegativity: The density functional viewpoint. The Journal of Chemical Physics 68(8):3801–3807. https://doi.org/10.1063/1.436185
45. Iczkowski RP, Margrave JL (1961) Electronegativity. Journal of the American Chemical Society 83(17):3547–3551. https://doi.org/10.1021/ja01478a001
46. Gázquez JL, Cedillo A, Vela A (2007) Electrodonating and electroaccepting powers. The Journal of Physical Chemistry 111(10):1966–1970. https://doi.org/10.1021/jp065459f
47. Parr RG, Pearson RG (1983) Absolute hardness: companion parameter to absolute electronegativity. Journal of the American Chemical Society 105(26):7512–7516. https://doi.org/10.1021/ja00364a005
48. Parr RG, Szentpály LV, Liu S (1999) Electrophilicity index. Journal of the American Chemical Society 121(9):1922–1924. https://doi.org/10.1021/ja983494x
49. Sharma V, Pahuja A, Srivastava S (2016) Spin-polarised DFT study of cobalt-doped gallium clusters. Molecular Physics 114(9):1472–1477. https://doi.org/10.1080/00268976.2015.1136004
50. Zhan L, Chen JZY, Liu W-K, Lai SK (2005) Asynchronous multicanonical basin hopping method and its applicationto cobalt nanoclusters. The Journal of Chemical Physics 122(24):244707. https://doi.org/10.1063/1.1940028
51. Rodríguez-Kessler PL, Rodríguez-Domínguez AR (2015) Stability of *Ni* clusters and the adsorption of CH_4: First-principles calculations. The Journal of Physical Chemistry C 119(22):12378–12384. https://doi.org/10.1021/acs.jpcc.5b01738
52. Fan HJ, Liu CW, Liao MS (1997) Geometry, electronic structure and magnetism of small Co_n (n= 2–8) clusters. Chemical Physics Letters 273(5):353–359. https://doi.org/10.1016/S0009-2614(97)00534-4
53. Rodríguez-López JL, Aguilera-Granja F, Michaelian K, Vega A (2003) Structure and magnetism of cobalt clusters. Physical Review B 67(17):174413. https://doi.org/10.1103/PhysRevB.67.174413
54. Datta S, Kabir M, Ganguly S, Sanyal B, Saha-Dasgupta T, Mookerjee A (2007) Structure, bonding, and magnetism of cobalt clusters from first-principles calculations. Phys Rev B 76(1):014429. https://doi.org/10.1103/PhysRevB.76.014429